SANDIA REPORT
SAND2012-1206
Unlimited Release
Printed February 2012

Interface Modeling to Predict Well Casing Damage for Big Hill Strategic Petroleum Reserve

Byoung Yoon Park and Brian L. Ehgartner

Prepared by
Sandia National Laboratories
Albuquerque, New Mexico 87185 and Livermore, California 94550

Sandia National Laboratories is a multi-program laboratory managed and operated by Sandia Corporation, a wholly owned subsidiary of Lockheed Martin Corporation, for the U.S. Department of Energy's National Nuclear Security Administration under contract DE-AC04-94AL85000.

Issued by Sandia National Laboratories, operated for the United States Department of Energy by Sandia Corporation.

Available to DOE and DOE contractors from
U.S. Department of Energy
Office of Scientific and Technical Information
P.O. Box 62
Oak Ridge, TN 37831

Telephone: (865) 576-8401
Facsimile: (865) 576-5728
E-Mail: reports@adonis.osti.gov
Online ordering: http://www.osti.gov/bridge

Available to the public from
U.S. Department of Commerce
National Technical Information Service
5285 Port Royal Rd.
Springfield, VA 22161

Telephone: (800) 553-6847
Facsimile: (703) 605-6900
E-Mail: orders@ntis.fedworld.gov
Online order: http://www.ntis.gov/help/ordermethods.asp?loc=7-4-0#online

SAND2012-1206
Unlimited Release
Printed February 2012

Interface Modeling to Predict Well Casing Damage for Big Hill Strategic Petroleum Reserve

Byoung Yoon Park[1] and Brian L. Ehgartner[2]

[1]-Geomechanics Department
Sandia National Laboratories
P.O. Box 5800
Albuquerque, NM 87185-MS0751

[2]-Geotechnology and Engineering Department
Sandia National Laboratories
P.O. Box 5800
Albuquerque, NM 87185-MS0706

Abstract

Oil leaks were found in well casings of Caverns 105 and 109 at the Big Hill Strategic Petroleum Reserve site. According to the field observations, two instances of casing damage occurred at the depth of the interface between the caprock and top of salt. This damage could be caused by interface movement induced by cavern volume closure due to salt creep. A three dimensional finite element model, which allows each cavern to be configured individually, was constructed to investigate shear and vertical displacements across each interface. The model contains interfaces between each lithology and a shear zone to examine the interface behavior in a realistic manner. This analysis results indicate that the casings of Caverns 105 and 109 failed by shear stress that exceeded shear strength due to the horizontal movement of the top of salt relative to the caprock, and tensile stress due to the downward movement of the top of salt from the caprock, respectively. The casings of Caverns 101, 110, 111 and 114, located at the far ends of the field, are predicted to be failed by shear stress in the near future. The casings of inmost Caverns 107 and 108 are predicted to be failed by tensile stress in the near future.

ACKNOWLEDGMENTS

This research is funded by SPR programs administered by the Office of Fossil Energy (FE) of the U.S. Department of Energy.

Dr. Courtney G. Herrick (SNL, Dept. 6211) and Dr. Stephen J. Bauer (SNL, Dept. 6914) provided a technical review and Dr. David J. Borns (SNL, Dept. 6912) provided a management review. This report has been improved by these individuals.

CONTENTS

FIGURES

TABLES

NOMENCLATURE

BH	Big Hill
D-P	Drucker-Prager
FEM	Finite Element Method
FE	Fossil Energy
MMB	Million Barrels
RF	Reduction Factor
SMF	Structural Multiplication Factor
SPR	Strategic Petroleum Reserve
UTM	Universal Transverse Mercator
WH	West Hackberry
WIPP	Waste Isolation Pilot Plant

1. INTRODUCTION

1.1. Background

Oil leaks were found at Big Hill (BH) Cavern Wells 105B and 109B by interpreting Caveman pressure data from Dyn McDermott [Ehgartner, 2010a; Ehgartner, 2011].

The Cavern 105B leak started after December 3rd, 2009, and had progressed to 8600 bbl on May 14, 2010 before the leak was brought under control by reducing cavern pressure. The rate increased both episodically and exponentially to over 150 bbl per day. The location of the leak is at about 1636 ft below the surface, which is close to the interface between the caprock and the salt dome.

The Cavern 109B leak started on October 8th, 2010. The total amount of oil leaked is estimated to be 2700 bbl. This occurred over an 88 day period resulting in an average leakage rate of 31 bbl per day. The location of the leak is at about 1630 ft below the surface at the joint.

1.2. Approach

This report attempts to find causes of the leaks through using numerical analysis. Previous three-dimensional finite element analyses were performed to evaluate the structural integrity of Strategic Petroleum Reserve (SPR) caverns located in BH salt dome [Park et al, 2005]. The cavern field was simplified using a 30-degree wedge model. The wedge model did not contain the interfaces between lithologies around the salt dome, and the fault (shear zone) that cuts across the overburden and caprock layers. The advanced model in this report is a full 3-D rendering of the site and includes the lithologic interfaces and the fault, needed to simulate motion between the caprock and the salt dome. The new model developed in this study considers actual geometries and locations of fourteen caverns and salt dome interfaces between the overburden and caprock; two caprock lithologies; caprock and salt dome; dome and surrounding rock, and a fault in the overburden and caprock layers. The shear displacement and vertical strain above the center of each cavern in the interface between caprock and salt dome will be calculated and compared to the field data. The evolution of the shear displacement and vertical strain will be investigated.

2. FIELD OBSERVATIONS

2.1. Oil Leak

The oil leak in Cavern 105 was first noticed in the Caveman† monitoring program when the predicted cavern pressurization rate departed significantly from the measured cavern pressures [Ehgartner, 2010a]. Figure 1 compares the measured pressure data (blue) to the predicted values (pink) using a status variable (yellow). A status variable outside the range 1 to -1 correlates to a statistical departure in expected cavern behavior of more than 3 standard deviations. In Figure 1, the leak becomes evident at the start of the last pressure cycle and grows with time. The difference between measured and predicted pressure is a discrepancy caused by the leak and thus can be used to estimate the amount of oil leaked from the well by simply multiplying it by the cavern compressibility. Caveman estimates the compressibility as 76 bbl/psi. Figure 2 provides estimates of the number of barrels of oil leaked to the formation with time. Approximately 8600 bbl of oil were lost through the well damage located at the salt/caprock interface. The leakage stopped when the cavern pressure was reduced to a level equal to or less than the formation spill pressure at the leak.

Figure 3 shows the difference between measured and predicted pressures in Cavern 109 [Ehgartner, 2011]. The measured pressure becomes discrepant after October 8, 2010, the assumed start of the leak. The total amount of leaked oil is estimated to be 2707 bbl. This occurred over an 88 day period resulting in an average leakage rate of 31 bbl/day.

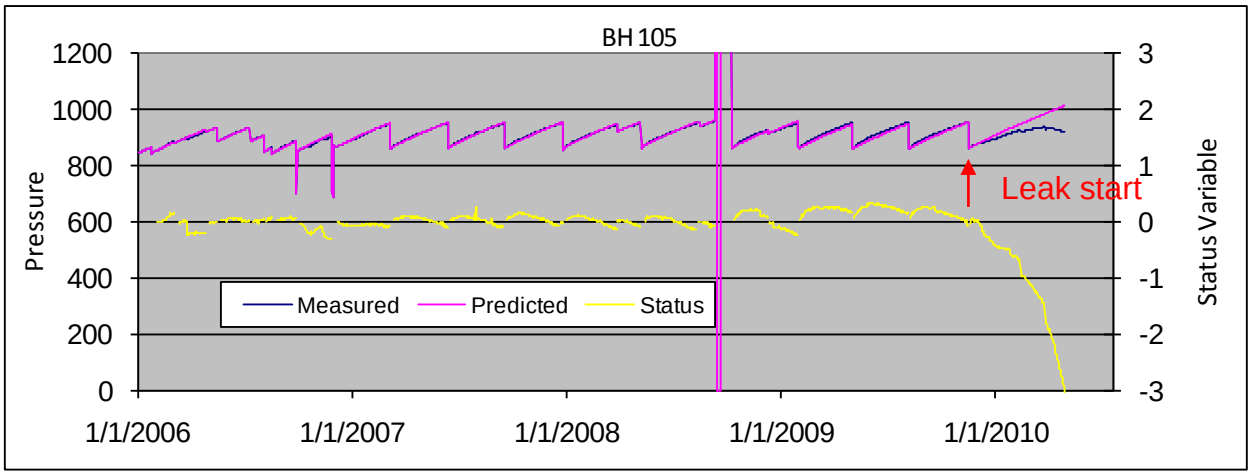

Figure 1: Comparison of expected and measured pressures in Cavern 105 [Ehgartner, 2010a].

† SPR cavern pressure analysis code developed by Sandia National Laboratories.

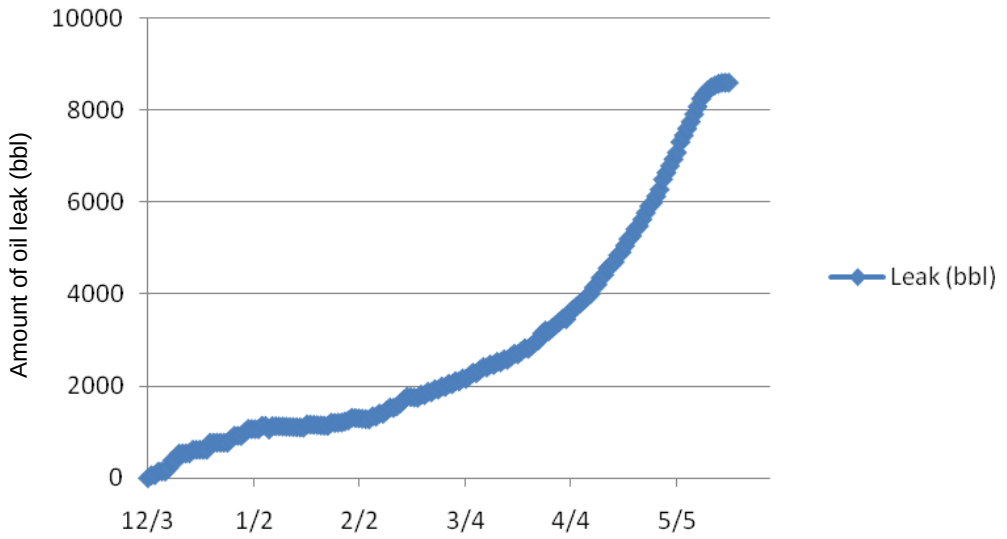

Figure 2: Calculated amount of oil leaked to the formation from Cavern 105 [Ehgartner, 2010a].

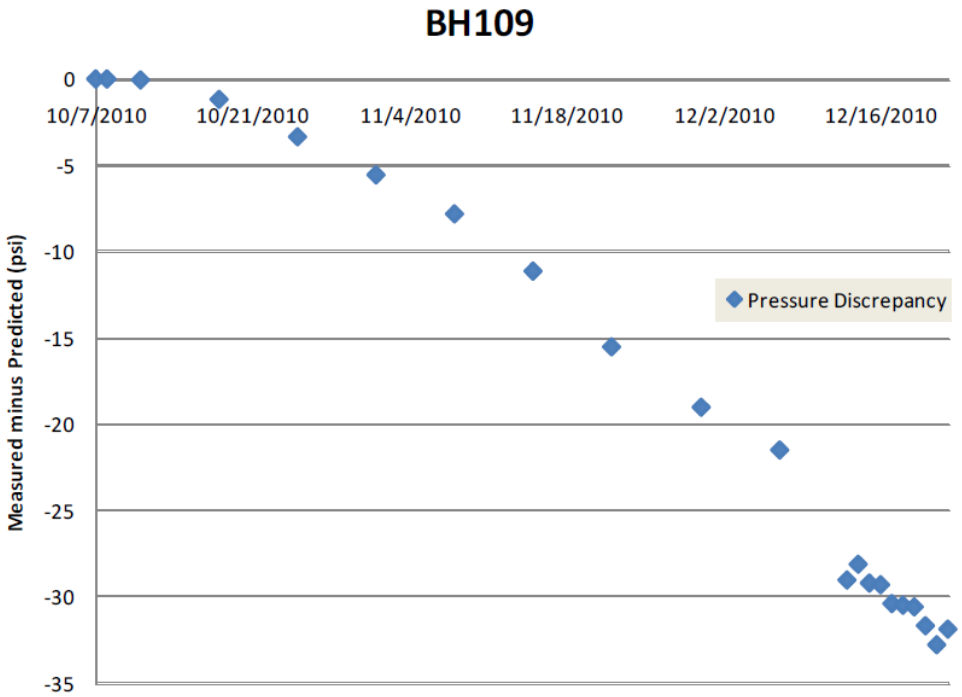

Figure 3: Difference between measured and predicted pressures in Cavern 109 [Ehgartner, 2011].

2.2. Casing Damage

The caverns at Big Hill have two wells each. The "A" well is a slick hole, and the "B" well contains a hanging string into the brine pool. While the leak necessitated logging of the "B" wells in Caverns 105 and 109, the "B" wells have not yet been logged in the other caverns because it necessitates a workover. All of the slick wells have been logged at Big Hill.

Figure 4 shows the logging results of Weatherford Multi Arm Caliper survey inside 13-3/8" cemented casing of BH Well 105B performed on 06/11/2010; the enlargement at 1636 ft depth is interpreted to be casing damage. A contour image of the interval between 1628 ft and 1677 ft depth (Figure 5) shows localized enlargement of the borehole.

Figure 6 shows the logging results of a Weatherford Multi-Arm Caliper survey inside the 13-3/8" cemented casing of BH Well 109B performed on 06/10/2010. Figure 7 shows a contour image in the interval between 1630 ft and 1650 ft depth. We can see a joint buckled at 1630 ft depth on the well.

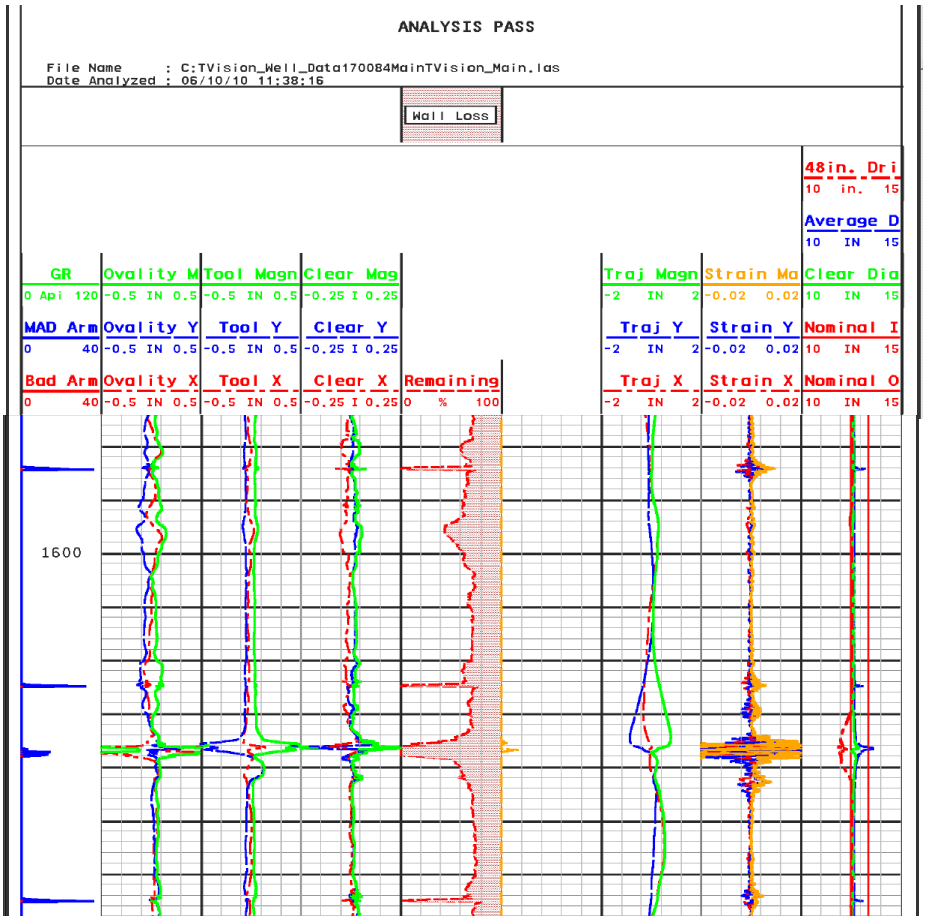

Figure 4: Multi-Arm Caliper survey logging plot of BH 105B (Each thick black line is 10 ft).

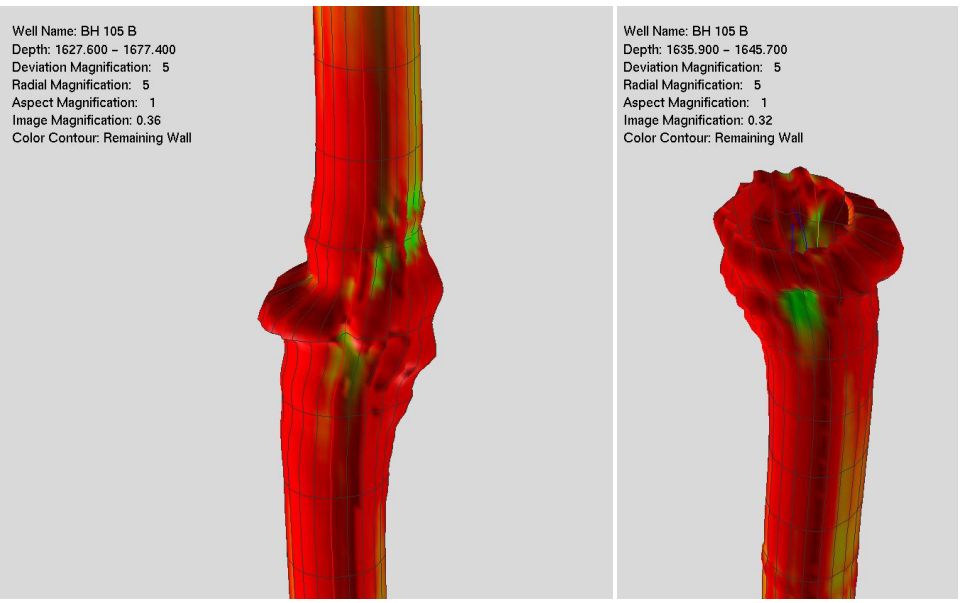

Figure 5: Contour image in depth 1628~1677 ft of BH 105B.

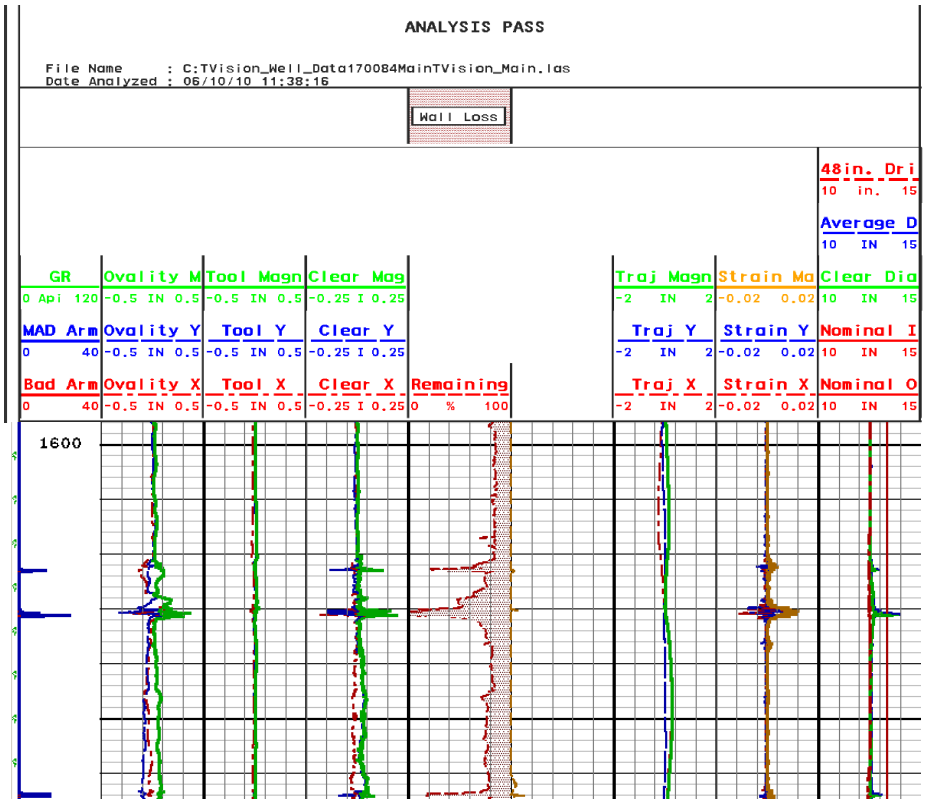

Figure 6: Multi-Arm Caliper survey logging plot of BH 109B.

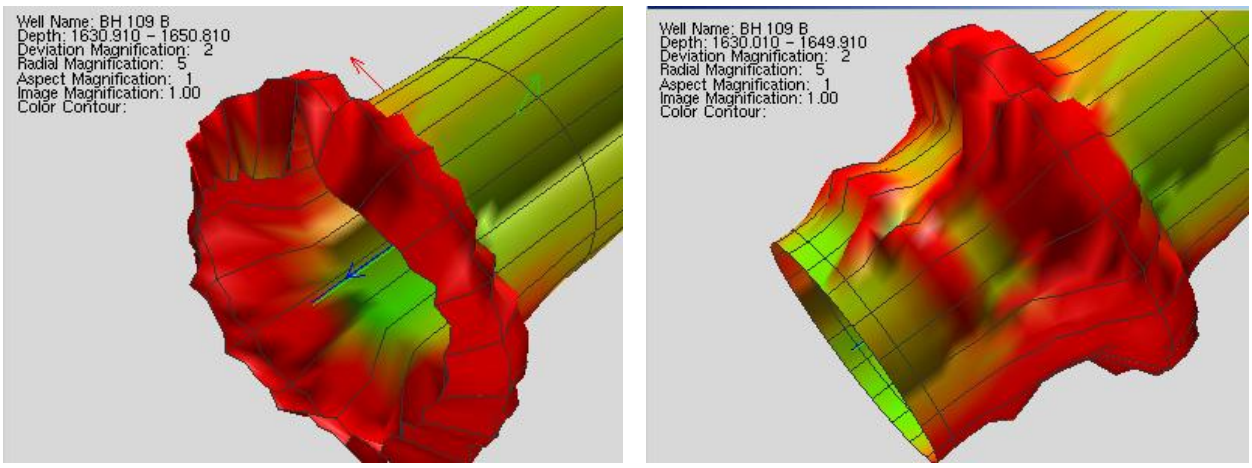

Figure 7: Contour image at 1628~1677 ft depth for BH 109B.

3. MODEL DESCRIPTION

3.1. Geomechanical Model

3.1.1. Salt dome geometry

Figure 8 shows a plan view of the BH site with contour lines defining the approximate location of the salt dome top. The locations for the 14 SPR currently in-use caverns (101-114) and five potential expansion caverns (X1-5) are shown. The figure also indicates the undeveloped area north of the DOE property line (Sabine Pass Terminal). The horizontal shape of the dome is approximately elliptical. The major and minor ellipse axes are measured as 7000 ft and 5800 ft, respectively.

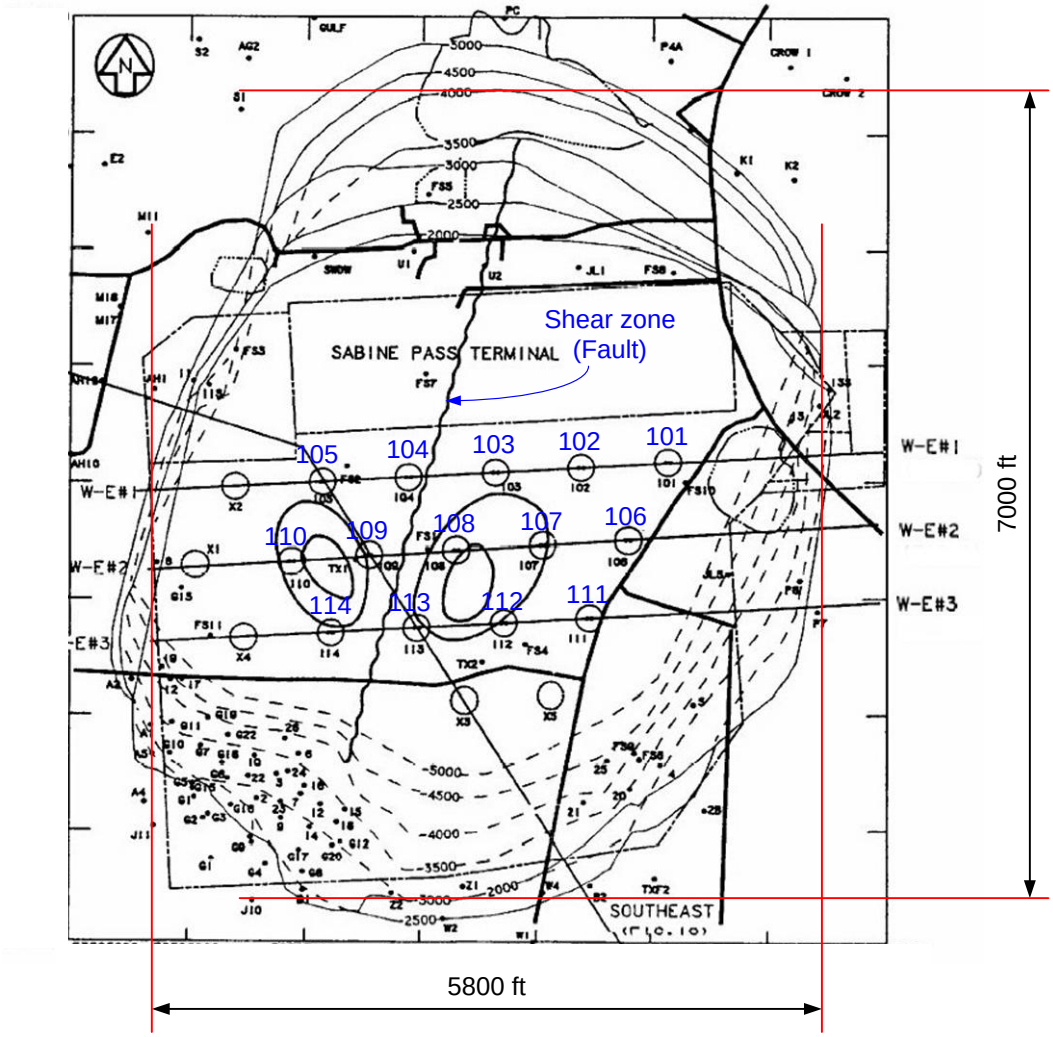

Figure 8: Big Hill site plan view [Magorian and Neal, 1988]

The West-East cross-section #1 through the northern-most row of caverns (Cavern 101-105) provides a geologic representation near the middle of the dome (Figure 9). The site has a thin overburden layer consisting of sand and soil and an exceptionally thick caprock sequence

comprised of two layers. The upper caprock is comprised mainly of gypsum and limestone, whereas the lower caprock is mostly anhydrite. A major fault extends approximately North-South along the entire length of the caprock and for an unknown depth into the salt. This fault zone has a pronounced effect on the subsidence measured above the site and is a consideration for future cavern placement [Ehgartner and Bauer, 2004].

Figure 10 shows a three dimensional representation of the BH salt dome constructed by digitally piecing together the separate models of the flank and top of salt. Figure 11 shows the salt dome with caprock as viewed from the northeast [Rautman et al, 2005]. For analysis purposes, the top layer of overburden is modeled as having a thickness of 300 ft, the upper caprock 900 ft thick, and the lower caprock 430 ft thick. The salt thickness over the caverns is approximately 660 ft. The bottom boundary of the present analysis model is set at 6000 ft below the surface.

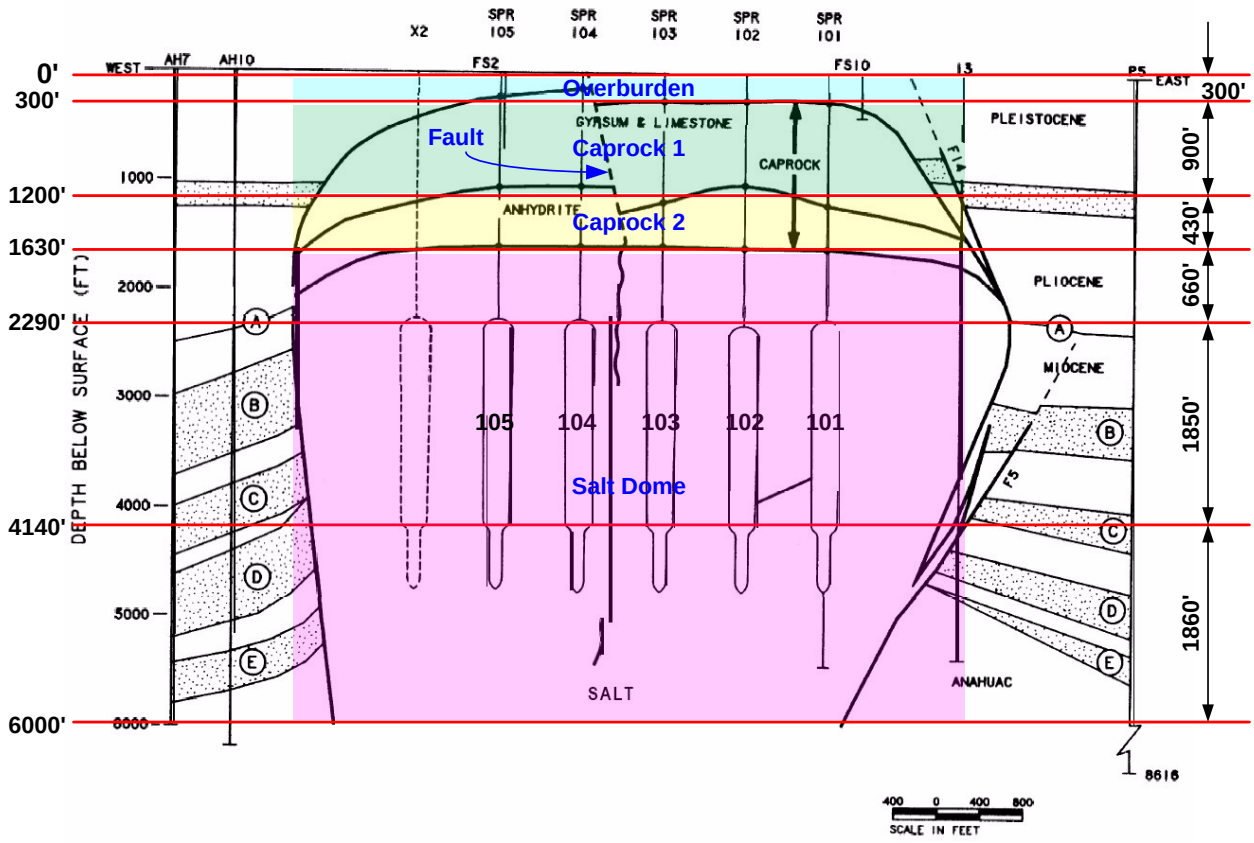

Figure 9: Cross-section (W-E #1 in Figure 8) near middle of dome [Magorian and Neal, 1988].

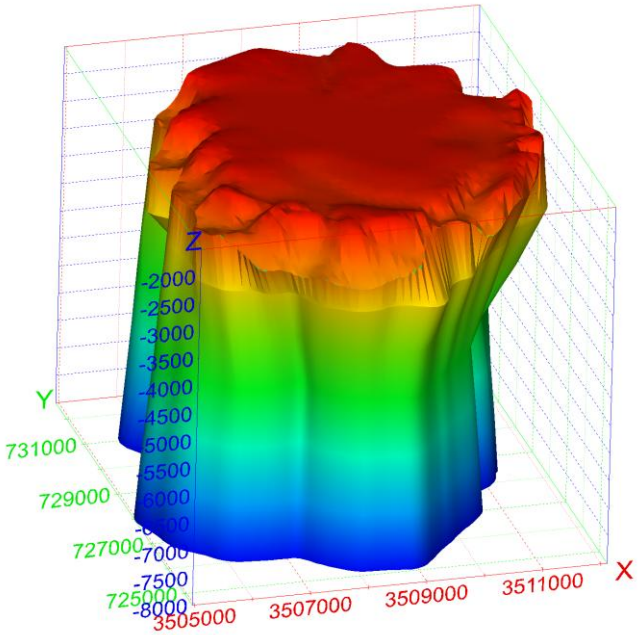

Figure 10: Three dimensional representation of the Big Hill salt dome [Rautman et al, 2005]. The color depicts the elevation. No overburden or caprock is shown.

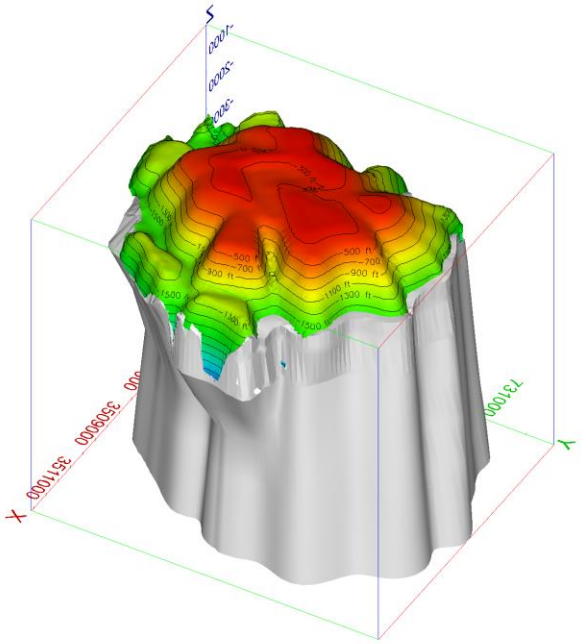

Figure 11: View of the caprock colored by elevation. The salt dome is shown in grey. View is from the northeast at an inclination of 40º from the horizontal [Rautman et al, 2005].

3.1.2. Salt Constitutive model and parameter values

Data for the creep constant, the stress exponent, and the thermal constant for the power law creep model used to describe the geomechanical behavior of the BH salt are very limited. Where needed, the data from the West Hackberry (WH) site has been used to augment the BH data, since both BH and WH salts are classified as soft salts [Munson, 1998] and are assumed mechanically similar for the purpose of this study. The salt data were derived through mechanical property testing of salt cores collected from boreholes [Wawersik and Zeuch, 1984]. The creep constitutive model considers only secondary or steady-state creep. The creep strain rate is determined from the effective stress as follows:

$$\dot{\varepsilon} = A\left(\frac{\sigma}{\mu}\right)^{n} \exp\left(-\frac{Q}{RT}\right) \tag{1}$$

where, $\dot{\varepsilon} =$ creep strain rate,
$\sigma =$ von Mises equivalent stress,
$\mu =$ shear modulus = E/2(1+ν), where E is Young's modulus and ν is Poisson's ratio
T = absolute temperature,
A = power law creep constant determined from back-fitting the model to creep data
n = stress exponent,
Q = effective activation energy,
R = universal gas constant.

The creep constant, A, in Eq. (1) is adjusted by a structural multiplication factor (SMF) which is used to match the volumetric closure of caverns. Through a number of back-fitting analyses [Park et al., 2005], a calibrated power law creep constant was determined. The values used as input data in the present analyses are listed in Table 1.

Table 1: Material properties of Big Hill salt used in the analysis:

Parameter	Unit	Value	Reference
Young's modulus (E)	GPa	31	Krieg, 1984
Density (ρ)	kg/m^3	2300	Krieg, 1984
Poisson's ratio (ν)		0.25	Krieg, 1984
Elastic modulus reduction factor (RF)		12.5	Magorian and Krieg, 1990
Bulk modulus (K)	GPa	1.653	from RF, E and ν
Two mu (2μ)	GPa	1.984	from RF, E and ν
Creep constant (A)	Pa$^{-4.9}$/s	5.79×10^{-36}	Krieg, 1984
Structure multiplication factor (SMF)		1.5	Park et al., 2005
Calibrated creep constant	Pa$^{-4.9}$/s	8.69×10^{-36}	Park et al., 2005
Stress exponent (n)		4.9	Krieg, 1984
Thermal constant (Q)	cal/mol	12000	Krieg, 1984
Universal gas constant (R)	cal/(mol·K)	1.9859	Mohr et al., 2011
Input thermal constant (Q/R)	K	6043	From Q and R

3.1.3. Lithologies around the salt dome

The surface overburden layer, which is mostly comprised of sand, is modeled as exhibiting elastic material behavior. The sand layer is considered isotropic and elastic, and has no assumed failure criteria. The upper caprock layer, consisting of gypsum and limestone, is also assumed to be elastic. Its properties are taken to be the same as those used for the WH analyses [Ehgartner and Sobolik, 2002]. The rock surrounding the salt dome is assumed to be isotropic, homogeneous elastic sandstone.

The anhydrite in the lower caprock layer is expected to experience inelastic material behavior. The anhydrite layer is considered isotropic and elastic until yield occurs [Butcher, 1997]. Once the yield stress is reached, plastic strain begins to accumulate. Yield is assumed to be governed by the Drucker-Prager (D-P) criterion:

$$\sqrt{J_2} = C - aI_1 \tag{2}$$

where, $I_1 = \sigma_1 + \sigma_2 + \sigma_3 = 3\sigma_m$: the first invariant of the stress tensor; $\sqrt{J_2} = \sqrt{\frac{(\sigma_1 - \sigma_2)^2 + (\sigma_2 - \sigma_3)^2 + (\sigma_3 - \sigma_1)^2}{6}}$: the square root of the second invariant of the deviatoric stress tensor; σ_1, σ_2, and σ_3 are the maximum, intermediate, and minimum principal stresses, respectively; σ_m is the mean stress; C and a are D-P constants.

However, the material properties of the BH anhydrite are unknown. Therefore, the behavior of the BH anhydrite is assumed to be the same as the Waste Isolation Pilot Plant (WIPP) anhydrite. A non-associative flow rule is used to determine the plastic strain components. To use the soil and foam model for the lower caprock, JAS3D input parameters are derived from the elastic properties and the D-P constants, C and a [Park et al., 2005]. The material properties including determined values (bold font) through back-fitting analyses in Table 1 and 2 are used as input data for JAS3D.

Table 2: Material properties of lithologies around salt dome used in the analyses.

	Unit	Overburden (Sand)	Caprock 1 (Limestone)	Caprock 2 (Anhydrite)	Surrounding Rock (Sandstone)
Young's modulus	GPa	0.1	**21**	75.1	**70**
Density	kg/m^3	1874	2500	2300	2500
Poisson's ratio	0.25	0.33	0.29	0.35	0.33
Bulk modulus	GPa	N/A	N/A	83.44	N/A
Two μ	GPa	N/A	N/A	55.63	N/A
A_0	MPa	N/A	N/A	2338	N/A
A_1		N/A	N/A	2.338	N/A
A_2		N/A	N/A	0	N/A

3.2. Interfaces and Fault Model

To investigate causes of well casing damage between the salt dome and the caprock, horizontal shear displacements and vertical strains at the interface need to be examined. Thus, interface blocks, special purpose analysis tools, are used to represent the interfaces between overburden and caprock 1; caprock 1 and caprock 2; caprock 2 and salt dome; surrounding rock and dome. The material behavior away from the interfaces is represented by material properties of caprock 1, caprock 2, and salt. The fault, which was ignored for the simplification in previous analyses [Park et al., 2005], is included in this model to perhaps better represent the large scale deformation considered in this study.

There is no interface geometry and material property data obtained from the field. The interfaces and fault are assumed to mechanically behave like sand, thus the overburden material properties (Table 2) are used in the analysis for the interfaces and fault. In geology and related fields, a stratum (plural: strata) is a layer of sedimentary rock or soil with internally consistent characteristics that distinguish it from other layers. The "stratum" is the fundamental unit in a stratigraphic column and forms the basis of the study of stratigraphy. Strata are typically seen as bands of different colored or differently structured material exposed in cliffs, road cuts, quarries, and river banks. Individual bands may vary in thickness from a few millimeters to a kilometer or more. In this study, the thicknesses of the interface materials are assumed to be a uniform 14 ft based on the largest vertical distances measured in Table 1 in Appendix I. The thickness of fault varies from a millimeter to a hundred meters with fault displacement (Figure 12). In this study, the fault thickness is assumed to be a uniform 14 ft as the thicknesses of interfaces for the simplification. These model attributes were incorporated into the finite element method (FEM) mesh described in Chapter 4.

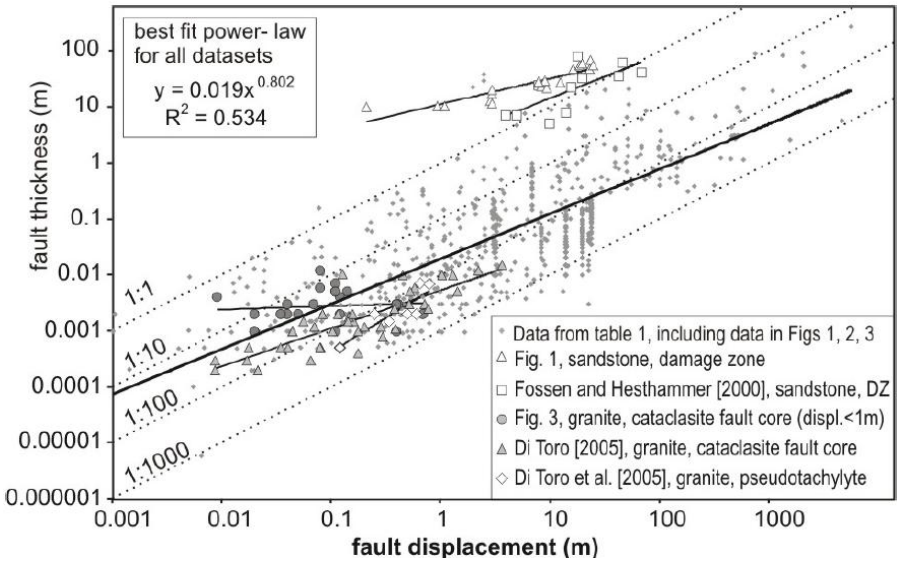

Figure 12: Log-log plot of a compilation of 16 fault thickness datasets reported in the literature including the data used by Hull [1988], and the three datasets in Shipton, et al. [2006].

3.3. Cavern Model

3.3.1. Cavern geometry and layout

The cavern shapes are approximately cylindrical and the cavern array is regular as shown in Figure 13. The cavern dimensions used in the model are simplified and are listed in Table 3 based on the sonar data. The completion date for the initial leach of each cavern is also listed. The X- and Y-coordinates for the center of each cavern were calculated by subtracting the Universal Transverse Mercator (UTM) coordinates of the center of the dome from UTM coordinates of each cavern. That is, the origin for the coordinate system of the model is the center of the dome.

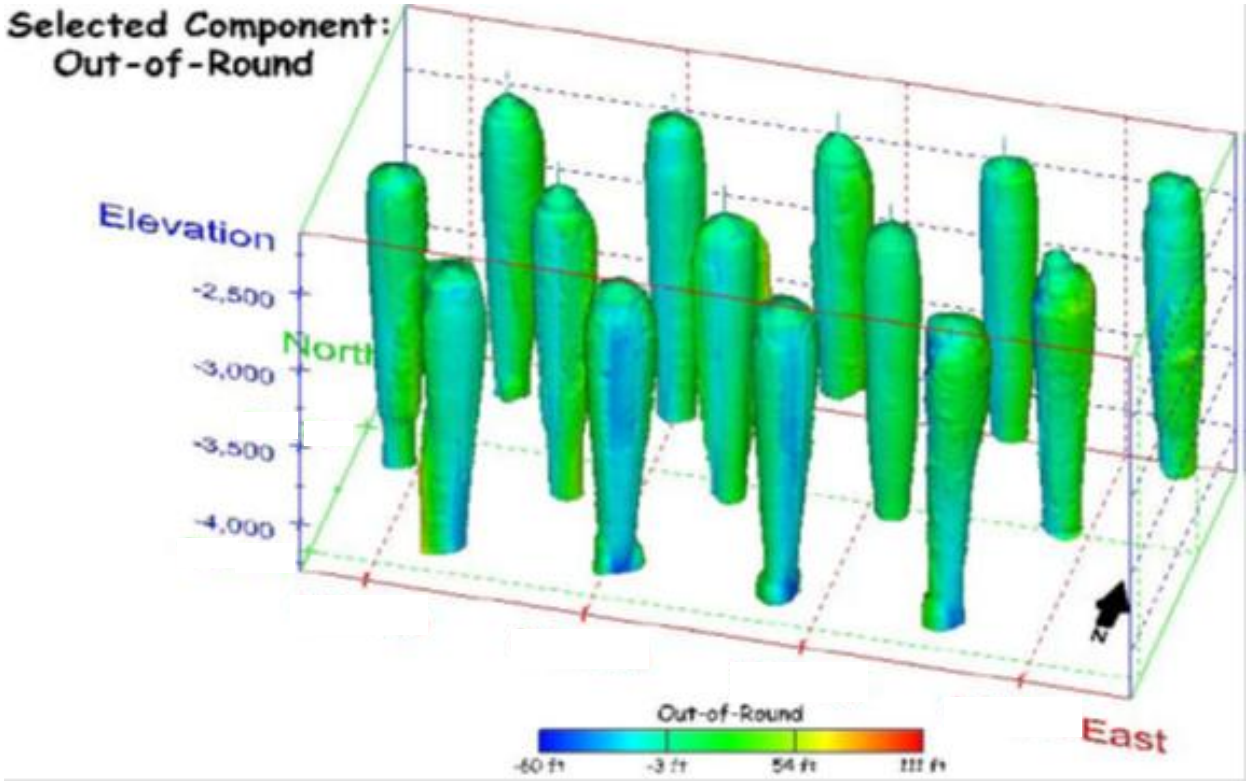

Figure 13: Perspective view of the entire cavern field at the Big Hill SPR site from the southeast [Rautman and Lord, 2007].

Table 3: Geometric parameters and initial leach completion dates for the fourteen extant caverns.

Cavern ID	X (East)	Y (North)	Z (Vertical Center)	Diameter	Radius	Cavern Top	Cavern Bottom	Cavern Height	Leach Completion Date
	ft	ft	ft	ft	ft	ft	ft	ft	mm/dd/yyyy
101	1875	-551	-3215	220	110	-2290	-4140	1850	9/18/1990
102	1125	-551	-3215	220	110	-2290	-4140	1850	10/21/1990
103	375	-551	-3215	220	110	-2290	-4140	1850	11/28/1990
104	-375	-551	-3215	220	110	-2290	-4140	1850	10/21/1990
105	-1125	-551	-3215	220	110	-2290	-4140	1850	11/11/1990
106	1500	-1200	-3215	220	110	-2290	-4140	1850	10/16/1990
107	750	-1200	-3215	220	110	-2290	-4140	1850	4/24/1990
108	0	-1200	-3215	220	110	-2290	-4140	1850	6/14/1990
109	-750	-1200	-3215	220	110	-2290	-4140	1850	7/24/1990
110	-1500	-1200	-3215	220	110	-2290	-4140	1850	4/19/1990
111	1124	-1849	-3215	220	110	-2290	-4140	1850	7/15/1991
112	374	-1850	-3215	220	110	-2290	-4140	1850	6/19/1991
113	-376	-1849	-3215	220	110	-2290	-4140	1850	5/1/1991
114	-1126	-1849	-3215	220	110	-2290	-4140	1850	8/29/1991

3.3.2. Model history

The caverns were leached from April 1990 through August 1991 as listed in Table 3. To simplify the model history for the purposes of the present simulation, it is assumed that all existing caverns were initially leached in 1990, which is considered time $t = 1$ year in the simulation. The analysis simulates caverns that were leached to full size over a one year period by means of gradually switching from salt to fresh water in the caverns. It was assumed that the SPR caverns were filled with petroleum one year after their initial leaches start. The caverns are simulated as creeping for thirty years. The simulation then performs oil drawdowns in the SPR caverns.

Every five years after the 31st year from the beginning of the simulation, every SPR cavern is modeled as being instantaneously leached. Modeling of the drawdown process of the caverns is performed by deleting elements along the walls of the caverns so that the volume is increased by 16% over the current volume. Leaching is assumed to occur uniformly along the entire height of the cavern. However, leaching is not permitted in the floor or roof of the caverns. The 5-year period between each drawdown allows the stress state in the salt to return to a steady-state condition, as will be evidenced in the predicted closure rates. The simulation will continue until the 5th drawdown is completed to examine the evolution of the shear displacement and vertical strain in the interfaces for a total of 56 years. Creep closure is allowed to occur in all caverns during the simulation period.

To investigate the cause of oil leaks and evaluate the other casings at the site, the slick well casing above the caverns were recently inspected with Weatherford multi arm caliper. The time frame for the multi arm caliper (present day) corresponds to approximately 21 years of simulation time and corresponding analysis results will be compared to the field inspection data. Figure 14 shows the time sequence for this study of the BH site, including the initial cavern leaching and the five drawdown leaches modeled in the simulation.

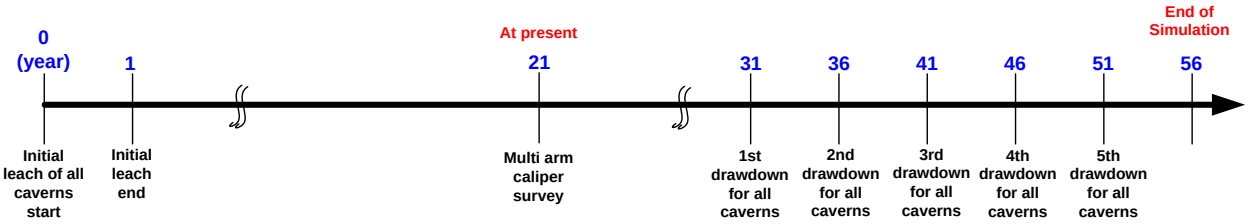

Figure 14: Time sequence for the simulation.

The pressure condition applied to each cavern is based on an average wellhead pressure of 905 psi which occurs when the wells are operated at normal or static conditions. An analysis of cavern pressures at BH between the years 1990 to 2010 indicates a cavern is pressurized within its normal operating range 74% of the time (1351 days during each five year period between drawdown leaches). Other operations, such as fluid transfers and workovers, require lower cavern pressures as shown in Table 4. Recently, operations have been improved to minimize low cavern pressures to assist in reducing volumetric losses due to creep [Ehgartner, 2010b]. Therefore, pressure drops are periodically included to simulate times during workover conditions. For simulation purposes, the pressure drop to 0 psi within each cavern lasts for 3 months which is about 4.9% of the time (89 days) during each 5-year period.

Rather than complicating the analyses, the following assumptions were made for the workover scenario. To better simulate actual field conditions, not all caverns are in workover mode at the same time. Figure 14 shows the wellhead pressure histories for each cavern.

Workover scenario:

- A constant pressure (905 psi) indicating normal conditions is applied for the majority of the time (Figure 15).
- For workover conditions, the wellhead pressure is dropped to zero.
- Workover of Cavern 101 begins one year after the initial leach is completed. After that, workovers are performed on Caverns 102 through 114 in numerical order. Workovers begin as soon as the workover of the prior cavern is completed.
- Workover durations are 3 month for all caverns.
- This workover cycle is repeated every 5 years.
- For both normal and workover conditions, the caverns are assumed to be full of oil having a pressure gradient of 0.37 psi/ft of depth.
- Pressure due to the oil head plus the wellhead is applied on the cavern boundary during the normal operation.

Table 4: Days in five year period with internal pressure ranges.

Cavern	Internal Pressure			days in 5 year period		
	0 to 400 psi	400 to 800 psi	800 + psi	**workovers**	Fluid transfers	Normal operation
BH101	5.1%	22.7%	71.8%	**93**	415	1310
BH102	2.7%	16.7%	80.3%	**50**	305	1466
BH103	3.6%	20.1%	76.1%	**66**	366	1390
BH104	3.1%	21.9%	74.8%	**56**	400	1365
BH105	5.9%	16.7%	77.1%	**108**	304	1407
BH106	4.8%	16.1%	79.0%	**88**	294	1441
BH107	4.4%	20.5%	74.8%	**80**	374	1366
BH108	7.0%	20.1%	72.9%	**127**	366	1330
BH109	6.4%	20.1%	73.4%	**116**	366	1339
BH110	6.1%	30.6%	63.1%	**110**	558	1152
BH111	3.7%	14.4%	81.6%	**68**	264	1490
BH112	4.9%	24.2%	70.7%	**89**	441	1290
BH113	4.2%	29.8%	65.8%	**76**	544	1202
BH114	6.8%	17.8%	75.1%	**124**	325	1371
Average	4.9%	20.8%	74.0%	**89**	380	1351

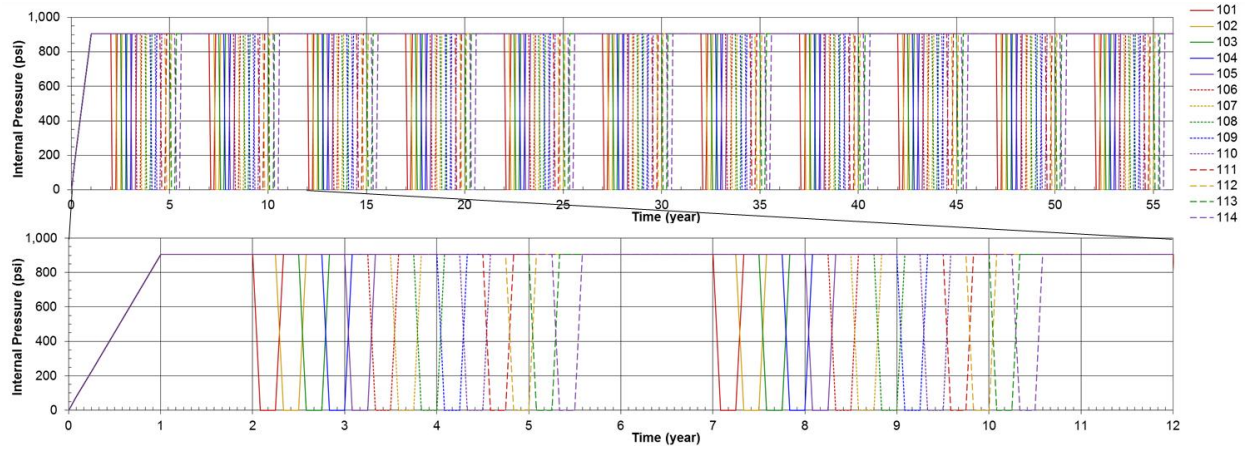

Figure 15: Wellhead pressure histories of each cavern.

3.4. Thermal Conditions

The finite element model includes a depth-dependent temperature gradient which starts at 76.7°F (24.84°C) at the surface and increases at the rate of 1.41°F/100ft (2.57°C/100m). The temperature profile is based on the average temperature data recorded in well logs from BH prior to leaching [Ballard and Ehgartner, 2000]. The temperature distribution is important because the creep response of the salt is temperature dependent. Radial temperature gradients due to cavern cooling effects from the cavern contents are not considered in these calculations. Previous 2D cavern studies have shown the predicted cavern deformation to be insensitive to the developed radial thermal gradients [Hoffman, 1992].

4. MESH

A three dimensional mesh, which allows each cavern to be configured individually, was constructed to investigate shear displacements and vertical strains in the interfaces. Figure 16 shows the overview of the finite element mesh of the stratigraphy and cavern field at BH. The mesh has been separated to show the individual material blocks. The X-axis of model is in the East direction, Y-axis is along the North direction, and Z-axis is the vertical direction, up being positive. The mesh consists of nineteen material blocks. Five blocks are used for Overburden, Caprock 1, Caprock 2, Salt Dome, and Surrounding Rock. Four blocks are used for the interfaces, and another four blocks are used for the fault. The other six blocks are used for the initial leach and five drawdown leaches for the fourteen caverns.

The Surrounding Rock block surrounds Caprock 1, Caprock 2, and Salt Dome. The interface block under Overburden is split off from the Overburden block. The thickness of every interface is 14 ft, thus the thickness of Overburden becomes 286 ft (= 300 ft – 14 ft). In the same manner, the interface under Caprock 1 is split off from the Caprock 1 block, thus the thickness of Caprock 1 becomes 886 ft. The interface under Caprock 2 is split off from the Caprock 2 block, thus the thickness of Caprock 2 becomes 416 ft. The interface surrounding Caprock 1, Caprock 2, and Salt dome is split off from the inside of the Surrounding Rock block, thus the radii of Caprock1, Caprock 2, and Salt Dome are not changed but the inside radius of Surrounding Rock decreases 14 ft.

The thickness of the fault (shear zone) is also assumed to be 14 ft. The strike direction and dip of the fault are 22º and 90º, respectively. The strike direction was approximated from Figure 8, and the dip was assumed to be vertical for the simplification. The fault runs between Caverns 103 and 104, Caverns 108 and 109, and Caverns 113 and 114. The fault is assumed to extend down to the top of Salt Dome from the surface.

The dome consists of Salt Dome, Caprock 1, and Caprock 2 is idealized to an elliptical cylinder with 7000 ft major (N-S), 5800 ft minor (E-W) diameters, and 5700 ft height (4370 ft salt dome height). Fourteen cavern blocks exist inside the Salt Dome block. All caverns are idealized to cylinders with 1850 ft height and 220 ft diameter. The cylinder blocks are surrounded by five onion ring blocks to idealize five drawdowns. The thickness of ring increases from inside to outside with 8.5, 9.1, 9.8, 10.6, and 11.4 ft to idealize 16% volume increments. The top of caverns is 660 ft down away from the top of salt (2290 ft below the surface).

Figure 17 shows the assembled mesh and the boundary conditions. The salt dome is modeled as being subjected to a regional far-field stresses acting from an infinite distance away. The lengths of the confining boundaries are 14,000 ft (two times the dome's major diameter) in the N-S direction and 11,600 ft (two times the dome's minor diameter) in the E-W direction. The mesh consists of 554,540 nodes and 545,580 elements with 19 element blocks, 6 node sets, and 84 side sets. The mesh was created using CUBIT‡ version 13.0.

‡ A mesh generation software copyrighted by Sandia Corporation.

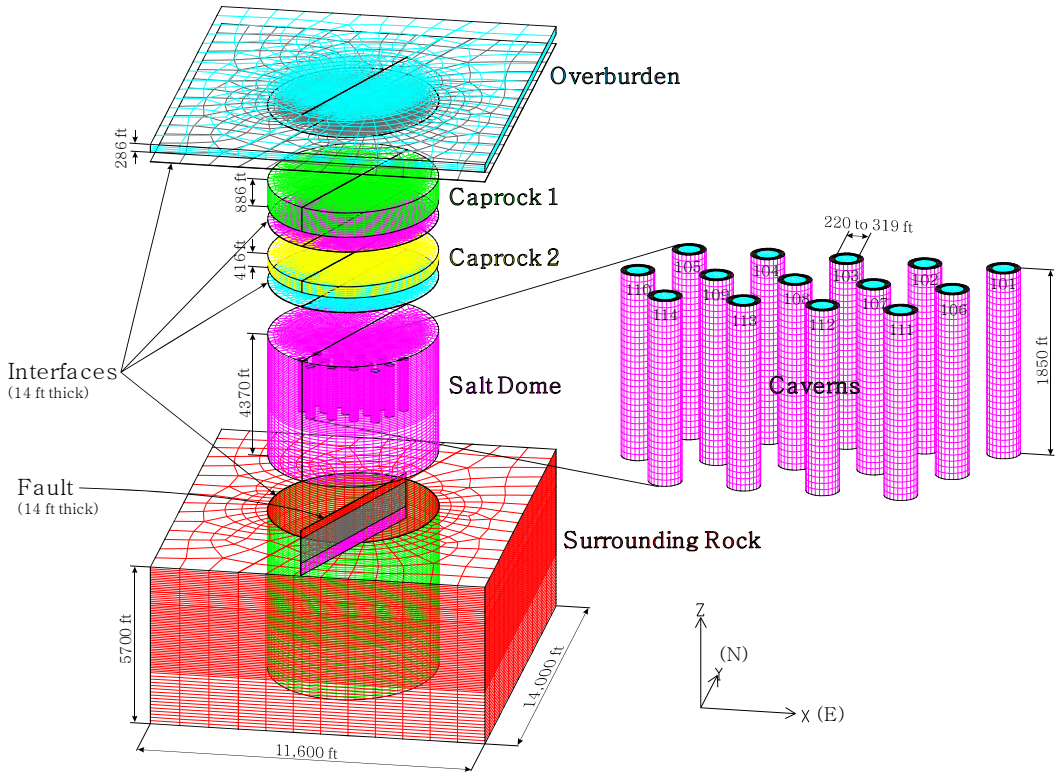

Figure 16: Overview of the finite element mesh of the stratigraphy and cavern field at Big Hill.

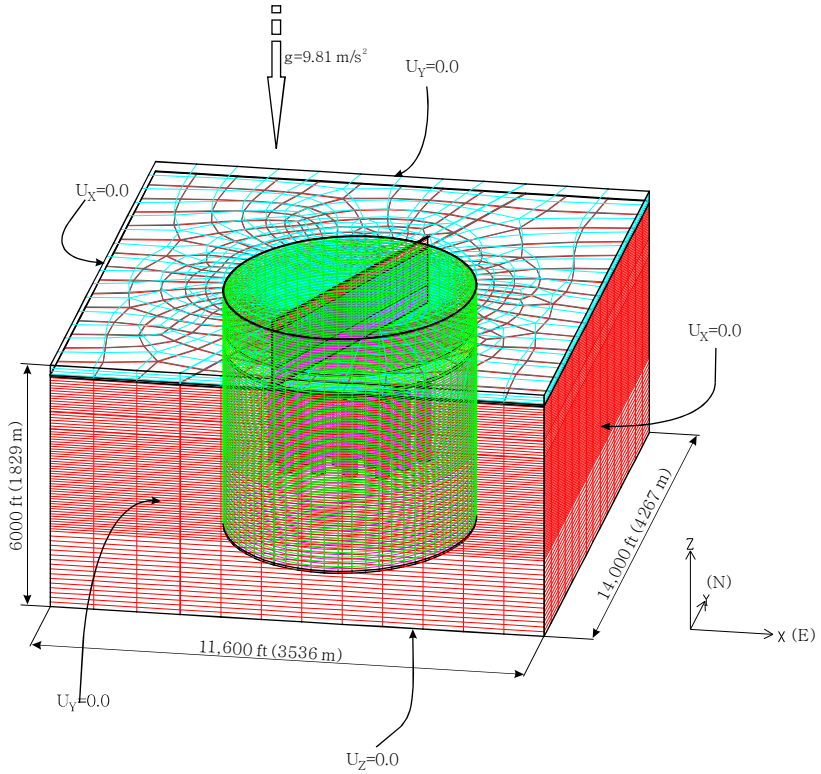

Figure 17: Finite mesh discretization and boundary conditions at Big Hill.

5. MODEL VERIFICATION

Figures 18 through 20 show comparisons the simulated volumetric closure of Cavern 101, 106, and 111, respectively, normalized by the initial cavern volume (i.e. cavern volume strain) with the field data. The slopes of lines are close to each other, i.e. the modeled volume closure rates match to the field data well. The peaks and the abrupt volume closures in the analysis results are caused by the workover scenarios in each cavern. They make a discrepancy between the analysis results and the field data, because the workover history for each cavern in the analysis is idealized with five year period. The predicted total volumetric closure normalized by total initial volume of fourteen caverns matches to the field data well as shown Figure 21. The peaks and abrupt volume closures of fourteen caverns are merged into one smooth line. This model approximation is reasonable to use to investigate the interface behavior because it is judged to represent the gross volume closure (strain) rather well. It is hypothesized that well casing damage at the interface would be caused by large scale salt rock mass movements brought about by cavern volume closure.

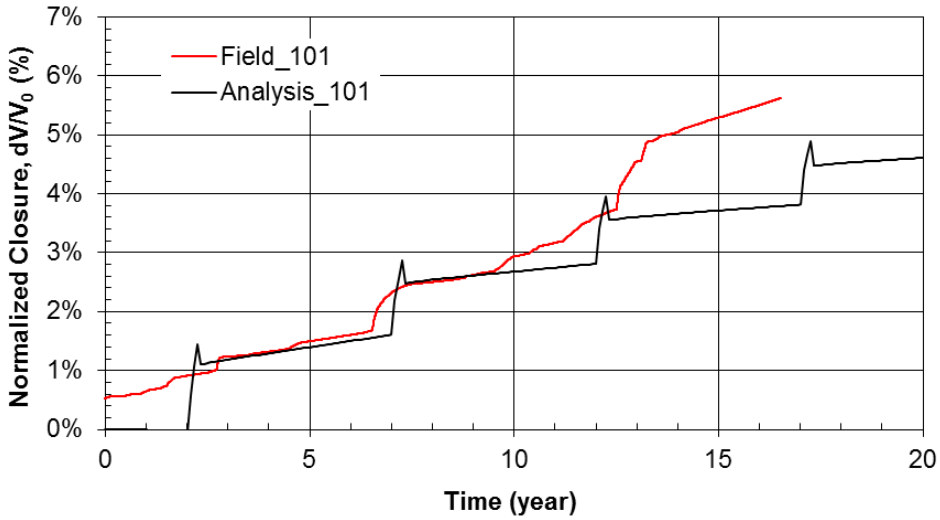

Figure 18: Comparison of predicted volumetric closure normalized by initial cavern volume for Cavern 101 with the field data.

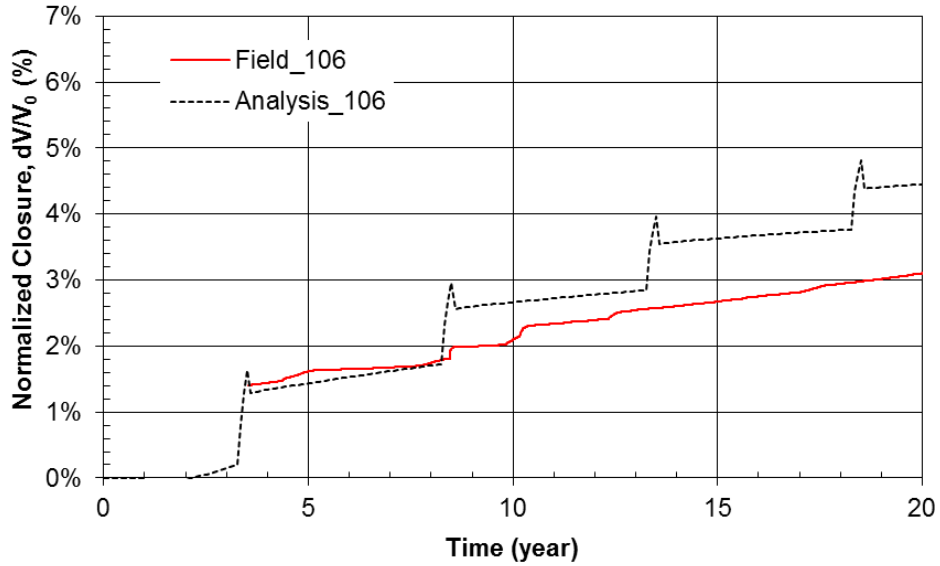

Figure 19: Comparison of predicted volumetric closure normalized by initial cavern volume for Cavern 106 with the field data.

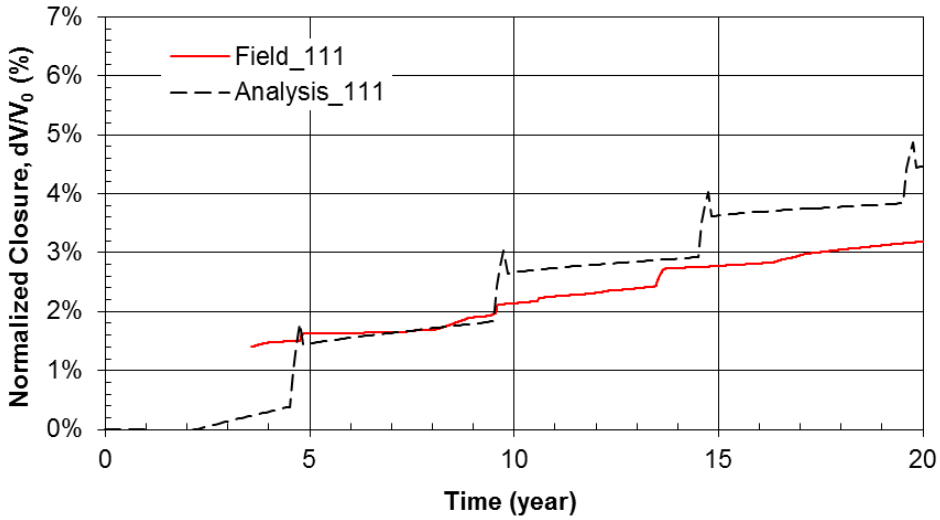

Figure 20: Comparison of predicted volumetric closure normalized by initial cavern volume for Cavern 111 with the field data.

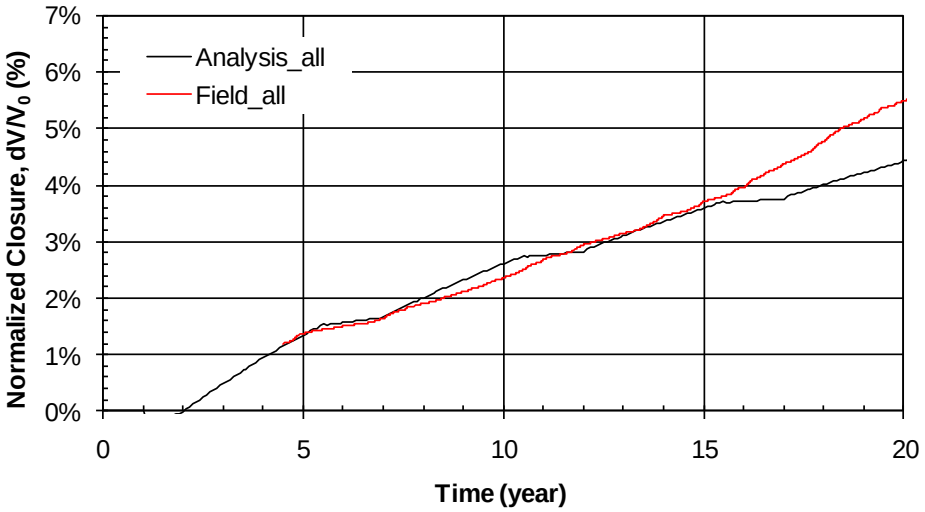

Figure 21: Comparison of predicted total volumetric closure normalized by total initial volume of the fourteen caverns with the field data.

6. ANALYSIS RESULTS

6.1. At Present, Twenty Years after Initial Leaching of the Caverns

Horizontal displacements and vertical distances in the interface between Caprock 2 and Salt Dome calculated during these FEM analyses are listed in Table 5 for year $t = 21$, which is twenty years after the initial leach is completed and represents calendar year 2010. The drawing in Figure 22 shows the denotation of each parameter in Table 5. The drawings in red and blue depict states at the initial leach of each cavern at $t = 0$ (1990) and at the inspection of each well casing $t = 21$ (2010), respectively. The bottom of Caprock 2 and the top of Salt Dome move downward with cavern volume closure due to salt creep. Node P_{S20} on the salt top above the center of each cavern moves horizontally in the direction of the predicted azimuth in Table 5 over 20 years of time.

The direction and magnitude of relative horizontal movement (movement of Node P_{S20} with a reference Node P_{C20}) on the salt top above the center of each cavern are shown in Figure 23**Error! Reference source not found.**. Every node above the fourteen caverns moves toward Cavern 108 over time. The horizontal node movement above Cavern 108 is predicted to be least (0.145 in) because Cavern 108 is located in the middle of fourteen caverns. On the other hand, the vertical stain above Cavern 108 is predicted to be most (8.6 millistrains) as listed in Table 5. These imply the well casing of Cavern 108 is relatively safe from horizontal shear failure, while having a higher possibility for vertical tensile failure. Figure 24 shows the vertical strain in the interface between Caprock 2 and Salt dome above the center of each cavern. The strains above Caverns 107, 108, and 109 are larger than others. The well casings above them could be failed by tensile stress. As mention in Chapter 2, the casing of BH Well 109B was failed at the joint (1630 ft depth) and oil leaked. The cause of failure could be a tensile stress created by the downward movement of salt dome top. Similar calculated vertical strain magnitudes suggest that the casings of BH Wells 107 and 108 may also fail by tensile stress in the near future.

Caverns 101, 105, 110, 111 and 114 make up a majority of the outermost caverns. The horizontal node movement above Cavern 114 is predicted to be most (2.645 in), while the vertical strain is predicted to be relatively small (5.3 millistrains). The vertical strain above Cavern 101 is predicted to be least (3.5 millistrain), while the horizontal node movement is predicted to be relatively large (2.493 in). These results imply the well casings above the outermost caverns have a greater chance of undergoing horizontal shear failure, while being relatively safe from the vertical tensile failure. Figure 25 shows the ratio of horizontal displacement of the node on the top of Salt Dome to vertical distance between Caprock 2 bottom and Salt dome top above the center of each cavern. The ratios above 101, 105, 110, 111, and 114 are larger than others. The well casings above them may fail by shear stress. As mention in Section 2, the casing of BH Well 105B had failed at 1636 ft depth and oil leaked. The cause of failure could be shear stress created by the horizontal movement of salt dome top.

Figure 26 through Figure 28 show the vertical strain contours above the caverns. The areas in red (failure limit is 0.81 millistrains based on the behavior of Cavern 109) indicate that well casing failure is imminently possible. The areas in the interface between Caprock 2 and Salt dome above Caverns 107, 108, and 109 appear red, i.e., the well casings in these areas may be in imminent danger of failing.

The BH logging results with the Weatherford Multi-Arm Caliper are provided in Appendix I. Table 1 in Appendix I shows the casings of 105B, 109A, 113A, 114A are classified as very high failure possible. The FEM analysis also gives a similar result. Therefore, we can anticipate what will happen to the well casings in the future from interpreting the analysis results from this study.

Table 5: Calculation results in the interface between Caprock 2 and Salt Dome at 20 years after initial leach.

Cavern ID	At bottom of Caprock 2			At top of Salt dome			Difference (ft)			Azimuth	Horizon	Vertical	Ratio	Vertical
	DA (ft)	DB (ft)	DC (ft)	DX (ft)	DY (ft)	DZ (ft)	TX	TY	TZ	(deg.)	Disp. (in)	Dist. (ft)	(in/ft)	Strain
101	0.089	-0.043	-0.620	-0.102	-0.125	-0.668	-0.191	-0.081	-0.048	246.9	2.493	14.048	0.18	0.0035
102	0.071	-0.043	-0.894	-0.063	-0.188	-0.980	-0.134	-0.144	-0.087	222.9	2.366	14.087	0.17	0.0061
103	0.041	-0.045	-1.076	-0.003	-0.219	-1.174	-0.044	-0.174	-0.097	194.3	2.159	14.097	0.15	0.0068
104	-0.030	-0.045	-1.057	0.057	-0.221	-1.154	0.088	-0.176	-0.097	153.6	2.359	14.097	0.17	0.0067
105	-0.052	-0.051	-0.851	0.119	-0.189	-0.926	0.171	-0.138	-0.075	128.9	2.633	14.075	0.19	0.0051
106	0.080	-0.067	-0.732	-0.110	-0.039	-0.816	-0.190	0.027	-0.083	278.2	2.305	14.083	0.16	0.0060
107	0.051	-0.072	-0.964	-0.050	-0.058	-1.083	-0.100	0.014	-0.119	277.9	1.214	14.119	0.09	0.0085
108	0.017	-0.077	-1.079	0.021	-0.065	-1.201	0.004	0.012	-0.122	17.3	0.145	14.122	0.01	0.0086
109	-0.052	-0.076	-0.960	0.090	-0.069	-1.076	0.141	0.007	-0.115	87.3	1.697	14.115	0.12	0.0081
110	-0.065	-0.073	-0.697	0.147	-0.064	-0.769	0.212	0.009	-0.072	87.5	2.543	14.072	0.18	0.0049
111	0.058	-0.091	-0.722	-0.078	0.069	-0.800	-0.137	0.161	-0.078	319.6	2.533	14.078	0.18	0.0056
112	0.024	-0.098	-0.876	-0.019	0.087	-0.975	-0.043	0.184	-0.099	346.8	2.272	14.099	0.16	0.0070
113	-0.003	-0.102	-0.913	0.045	0.083	-1.004	0.048	0.185	-0.091	14.5	2.288	14.091	0.16	0.0064
114	-0.061	-0.094	-0.721	0.103	0.053	-0.798	0.164	0.147	-0.076	48.2	2.645	14.076	0.19	0.0053

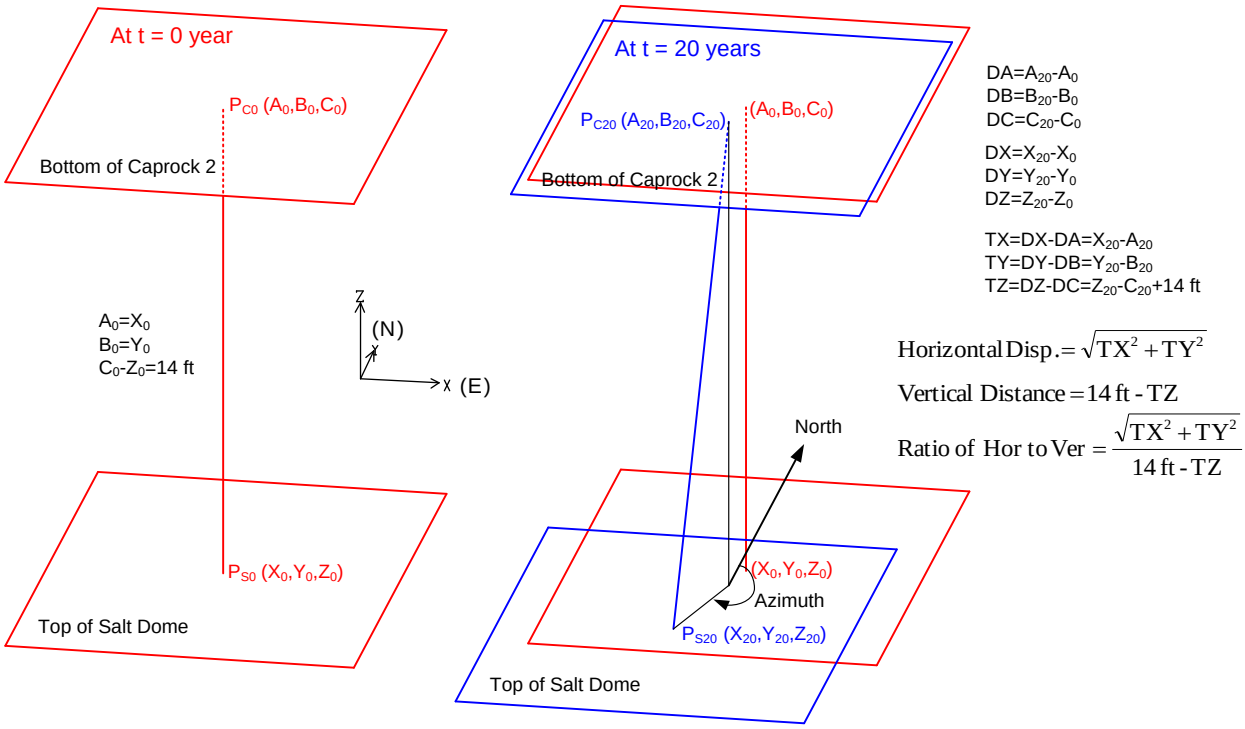

Figure 22: Denotation of the parameters in Table 5.

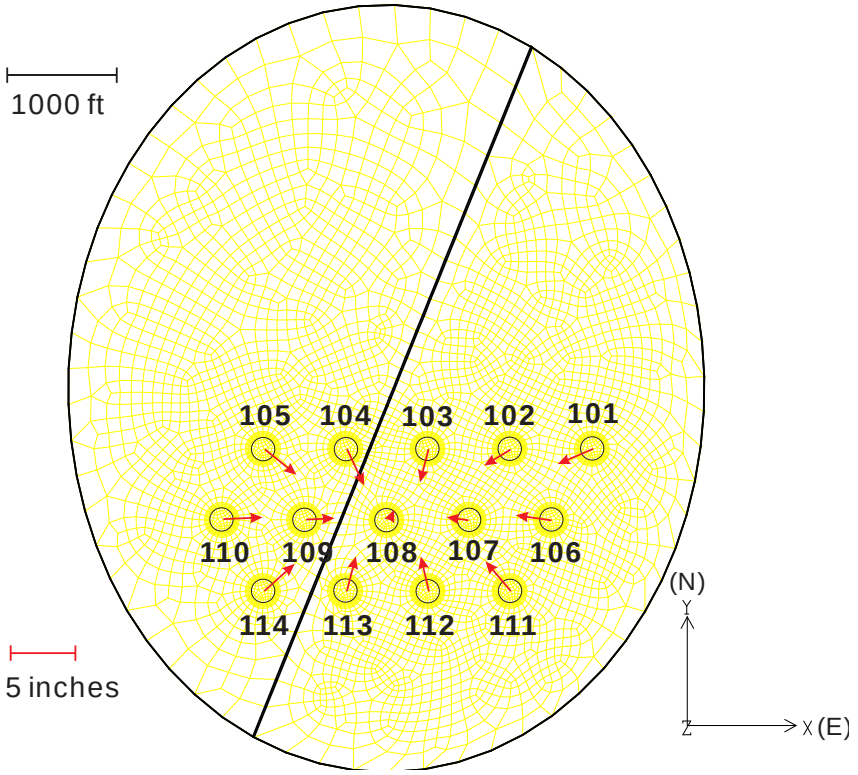

Figure 23: Direction and magnitude of horizontal movement on the salt top above the center of each cavern.

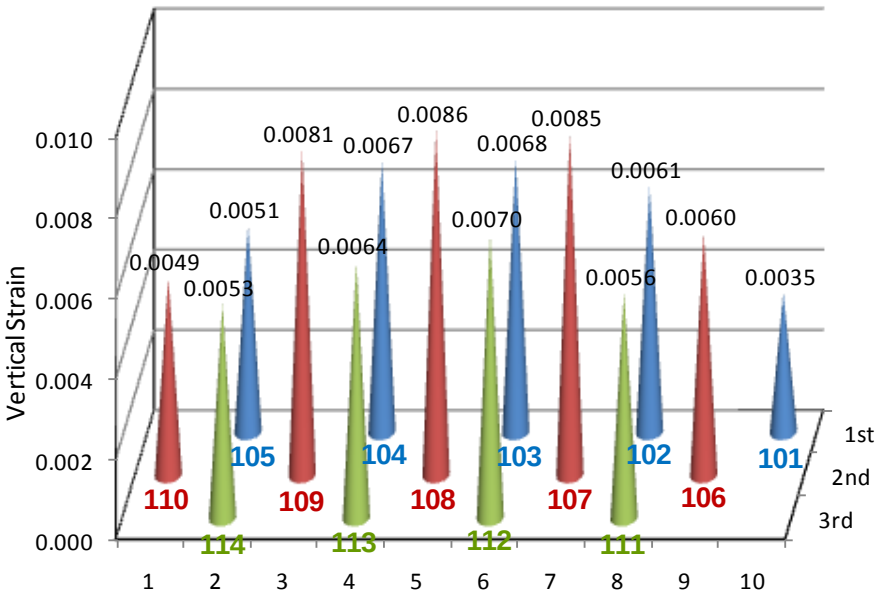

Figure 24: Vertical strain in the interface between Caprock 2 and Salt Dome above the center of each cavern.

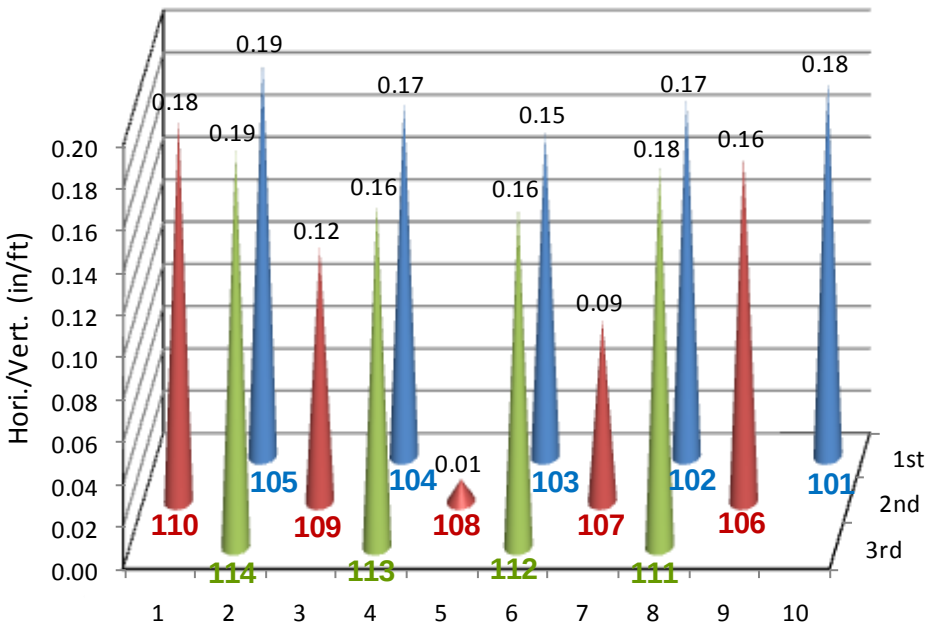

Figure 25: Ratio of horizontal displacement to vertical distance between Caprock 2 bottom and Salt Dome top above the center of each cavern.

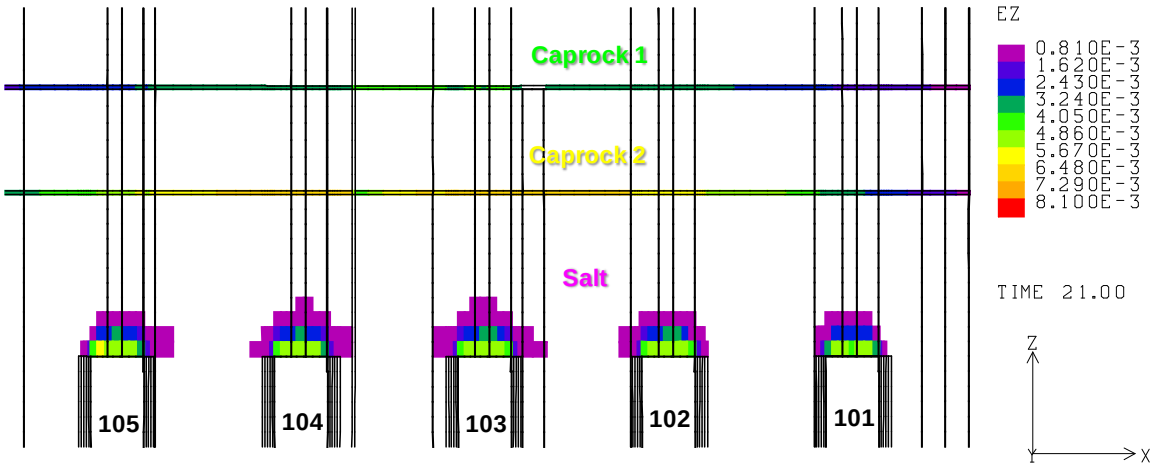

Figure 26: Vertical strain contours above Caverns 101 through 105 twenty years from completion of initial leach.

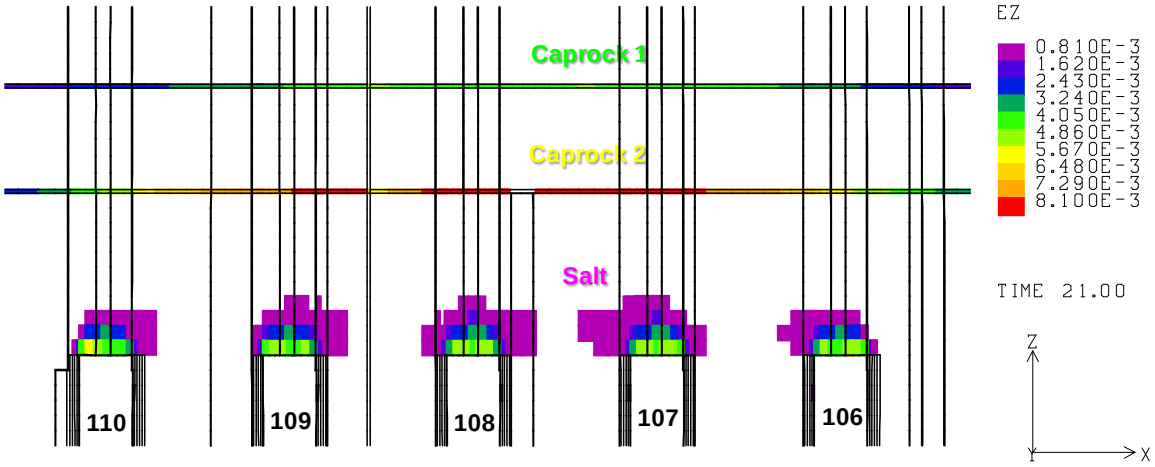

Figure 27: Vertical strain contours above Caverns 106 through 110 twenty years from completion of initial leach.

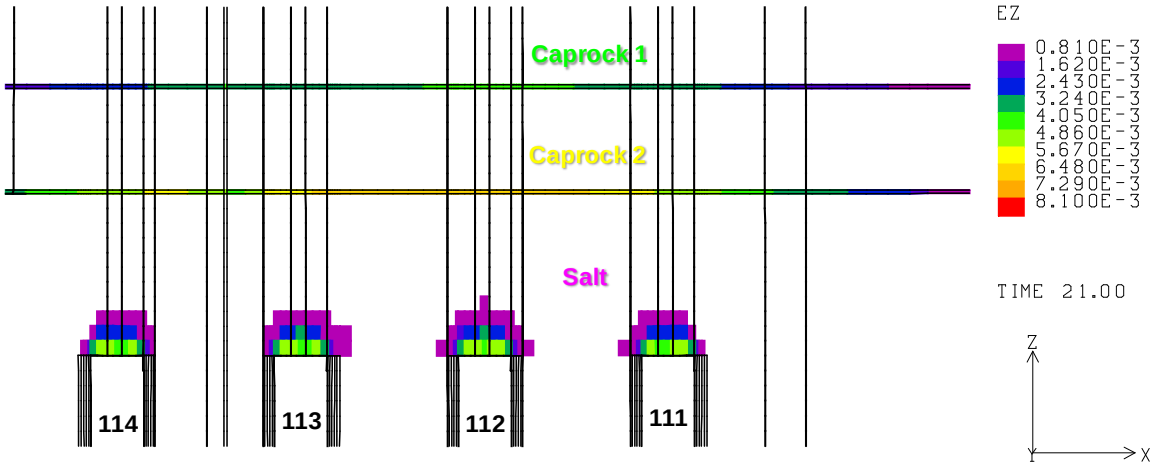

Figure 28: Vertical strain contours above Caverns 111 through 114 twenty years from completion of initial leach.

6.2. Predictions of future response

Figure 29 shows the ratio of relative horizontal movement (movement of node P_{S20} with a reference node P_{C20} in Figure 22) to vertical distance between Salt Dome top and Caprock 2 bottom above the center of each cavern over time. The well casing of Cavern 105 failed due to shear displacement at 20 years after the initial leach (2010) as mentioned in Section 6.1. The ratio was calculated to be 0.187 when the well casing failed. Therefore, the ratio of 0.187 can be used as for an approximate shear displacement failure limit (dash line in Figure 29). If this criterion is applicable to all the wells, the well casings of Caverns 103, 107, 108, and 109 are not predicted to fail due to shear displacement until 30 years after the initial leach (2020). In these analyses, leaching due to periodic 5 year drawdowns starts at 31 years. Table 6 lists the predicted time when the well casing of each cavern is predicted to fail due to shear displacement.

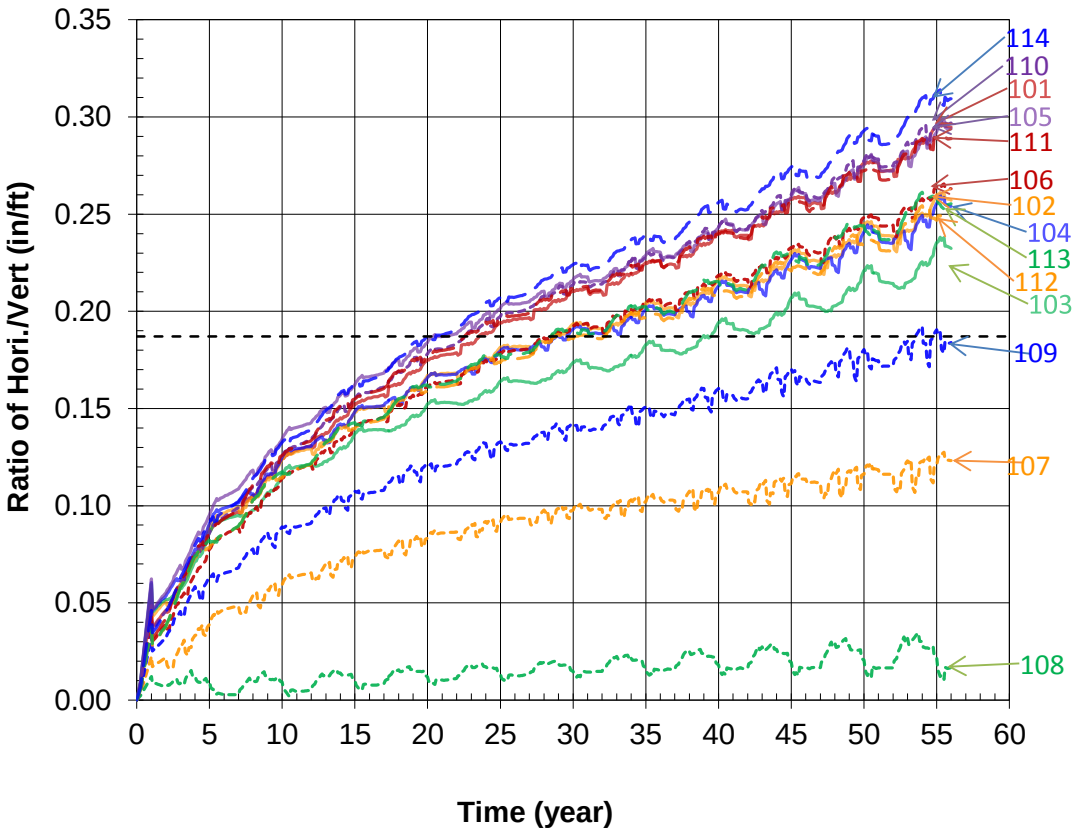

Figure 29: Ratio of relative horizontal displacement to vertical distance between Salt Dome top and Caprock 1 bottom.

Table 6: Predicted well casing fail date due to shear displacement.

Cavern	Predicted Well Casing Fail Date		Remark
	Since initial leach (year)	Date	
101	22.58	Jul-2012	May fail in near future
102	27.58	Jul-2017	
103	37.92	Nov-2027	Failure not predicted without drawdown
104	27.83	Oct-2017	
105	19.33	Apr-2009	Failed
106	27.58	Jul-2017	
107			Failure not predicted
108			Failure not predicted
109	52.58	Jul-2042	Failure not predicted without drawdown
110	21.58	Jul-2011	May fail in near future
111	21.50	Jun-2011	May fail in near future
112	27.83	Oct-2017	
113	27.50	Jun-2017	
114	19.00	Dec-2008	May fail in near future

Figure 30 shows the vertical strain as a function of time in the interface between Salt Dome and Caprock 2 above the center of each cavern. The well casing of Cavern 109 failed due to excessive vertical strain at 20 years after the initial leach done (2010) as mentioned in Section 6.1. The vertical strain was predicted to be 8.10 millistrains when the well casing of Cavern 109 was failed at the joint. Therefore, 8.10 millistrains may be used as a vertical strain failure limit (dash line in Figure 30). The well casings of Cavern 101, 102, 105, 106, 110, 111, 113, and 114 are not predicted to fail until 30 years after the initial leach (2020) due to excessive vertical strain. Table 7 lists the predicted time when the well casing of each cavern is predicted to fail due to vertical strain.

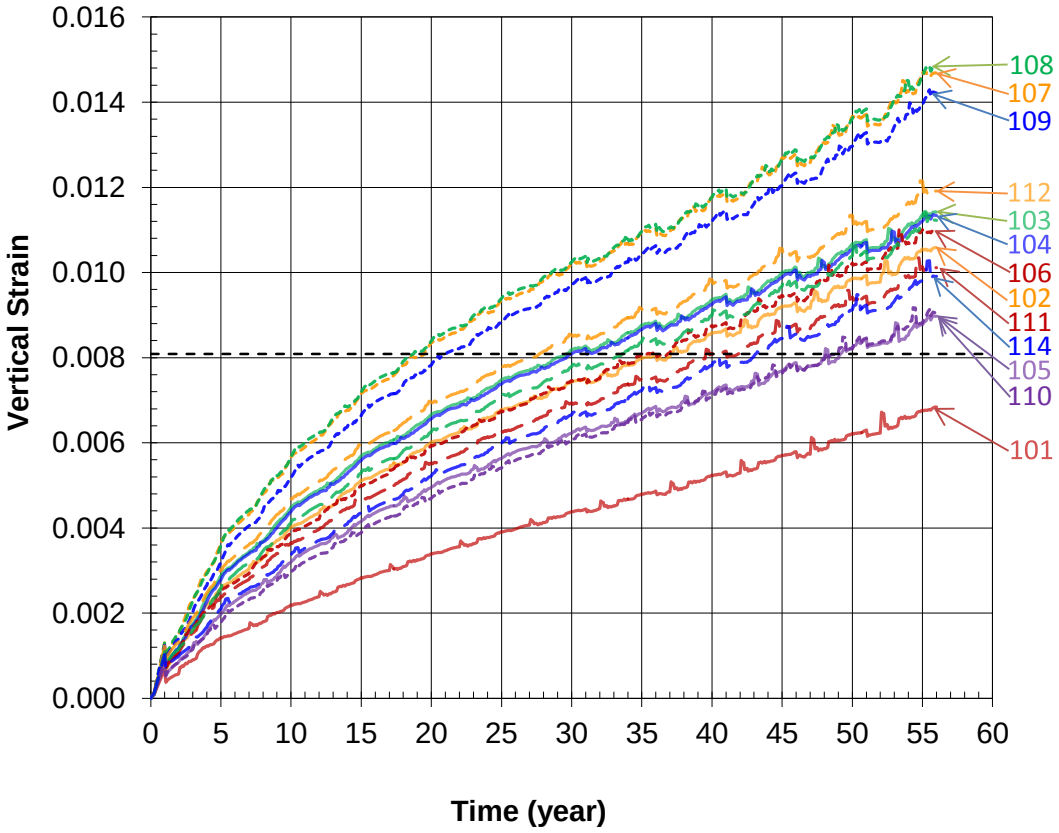

Figure 30: Vertical strain in the interface between Caprock 2 and Salt dome above the center of each cavern.

Table 7: Predicted well casing fail date due to vertical strain.

Cavern	Predicted Well Casing Fail Date		Remark
	Since initial leach (year)	Date	
101	> 56		Failure not predicted
102	36.08	Jan-2026	Failure not predicted without drawdown
103	28.67	Aug-2018	
104	29.08	Jan-2019	
105	47.08	Jan-2037	Failure not predicted without drawdown
106	34.00	Dec-2023	Failure not predicted without drawdown
107	18.58	Jul-2008	May fail in the near future
108	17.75	Sep-2007	May fail in the near future
109	20.00	Dec-2009	Failed
110	47.17	Feb-2037	Failure not predicted without drawdown
111	41.67	Aug-2031	Failure not predicted without drawdown
112	26.75	Sep-2016	
113	32.67	Aug-2022	Failure not predicted without drawdown
114	42.17	Feb-2032	Failure not predicted without drawdown

7. SUMMARY AND FUTURE WORK

Oil leaks were found at the well casings of Caverns 105 and 109 in BH SPR salt dome. According to the field observation, the casing damages occurred at the depth of the interface between the caprock and salt dome. To better understand the causes of this damage, a FEM analysis using a three dimensional mesh, which allowed each cavern to be individually represented, was undertaken to investigate shear displacements and vertical strains at the interfaces. The model contains interfaces between the lithologies and a shear zone to examine the interface behavior in a rigorous manner.

The causes of the damaged casing segments are a result of vertical and horizontal movements of the interface between the caprock and salt dome. The cavern volume closure due to salt creep produces movement between the salt top and caprock bottom. The displacement rates of the top and the bottom differ. This difference facilitates development of horizontal shear and vertical tensile stresses.

The nodes on the top of the salt layer move horizontally toward Cavern 108, which is located in the center of the fourteen caverns. The magnitudes of the horizontal movements above the outermost Caverns 101, 105, 110, 111 and 114 are larger than those of the other caverns. Using the horizontal displacement of the failed well of Cavern 105 as a failure criterion applicable to the other wells predicts that the well casings of Caverns 101, 110, 111 and 115 are in jeopardy of failing by shear stress in the near future.

On the other hand, the distances between nodes on the salt top and the caprock bottom above the center of each cavern increase over time. The increased distances above the inner Caverns 107, 108, and 109 are larger than others. Using the vertical displacement of the failed well of Cavern 109 as a failure criterion applicable to the other wells predicts that the well casings of Cavern 107 and 108 may be in imminent danger of failing by tensile stress due to excessive vertical strain.

Future work should consider additional forces that may be present at Big Hill. Currently, surface uplift has been occurring since 2002 in the eastern region of the Big Hill cavern field due to injection of liquid waste into the Newpark injection wells [Lord, 2011]. These injection wells are in close proximity to the Big Hill caverns. Five wells are actively being injected with waste, with the largest volumes being injected within the caprock in the southeastern region of the dome. Newpark injects approximately 2.4 MMB of liquid a year into the caprock. This injection impacts subsidence and caprock deformation. The well casings, therefore, would also be impacted by the injection. This current situation was not considered in this study.

A more sophisticated casing model would enable more accurate predictions of failure. For example, the failure models used above are simplistic as each mode (shear and vertical strain) is considered separately and based on a very limited sample size. In reality both modes are coupled to influence the strength of the casing. Also the well is comprised of two casings cemented into the salt, with additional casings cemented in the caprock and sand. The location of couplings within the multi-cased wells will likely influence the strength of the well.

Additionally, another model improvement may be formulated to treat the interface as a contact surface rather than simulated as discrete elements. While such algorithms exist they are troublesome to implement. None-the-less, utilizing contact surfaces could enhance the

predictions especially if the separation between surfaces accelerates due to the loss of cohesion as partings develop.

8. REFERENCES

Ballard, S. and B.L. Ehgartner, 2000, *CAVEMAN Version 3.0: System for SPR Cavern Pressure Analysis*, SAND2000-1751, Sandia National Laboratories, Albuquerque, NM 87185-0750.

Butcher, B.M. 1997. *A Summary of the Sources of Input Parameter Values for the WIPP Final Porosity Surface Calculations*, SAND97-0796, Albuquerque, NM: Sandia National Laboratories.

Ehgartner, B.L., 2010a, *Big Hill 105 Leak Analyses*, Memorandum from B. Ehgartner to R.E. Myers, DOE SPR PMO dated September 16, 2010. Sandia National Laboratories, Albuquerque, New Mexico.

Ehgartner, B.L., 2010b, *Ullage Losses*, Memorandum from B. Ehgartner to R.E. Myers, DOE SPR PMO dated October 27, 2010. Sandia National Laboratories, Albuquerque, New Mexico.

Ehgartner, B.L., 2011, *Big Hill 109B Leak Estimate*, Memorandum from B. Ehgartner to R.E. Myers, DOE SPR PMO dated February 18, 2011. Sandia National Laboratories, Albuquerque, New Mexico.

Ehgartner, B.L. and S.R. Sobolik, 2002. *3-D Cavern Enlargement Analyses*, SAND2002-0526, Sandia National Laboratories, Albuquerque, NM 87185-0706.

Hoffman, E.L., 1992, *Investigation of Analysis Assumptions for SPR Calculations*, memo to J. K. Linn dated February 7, 1992, Sandia National Laboratories, Albuquerque, New Mexico.

Hull, J., 1988. *Thickness-displacement relationships for deformation zones*, J. Struct. Geol., 10, 431-435.

Krieg, R. D., 1984, *Reference Stratigraphy and Rock Properties for the Waste Isolation Pilot Plant (WIPP) Project*, SAND83-1908, Sandia National Laboratories, Albuquerque, NM 87185.

Lord, A.S., 2011, Impact of Waste Injection Wells on Big Hill Subsidence, Draft memorandum from A.S. Lord to Gerard Berndsen, DOE SPR PMO dated June 21, 2011, Sandia National Laboratories, Albuquerque, NM 87185.

Magorian, T.R, and J.T. Neal, 1988. *Strategic Petroleum Reserve (SPR) Addition Geological Site Characterization Studies Big Hill Salt Dome, Texas*, SAND88-2267**,** Albuquerque, NM: Sandia National Laboratories.

Magorian, T.R., and R.D Krieg, 1990. Investigation of an Empirical Creep Law for Rock Salt that Uses Reduced Elastic Moduli. *Proc. 31st U.S. Symposium on Rock Mechanics, June 18-20, 1990*.

Mohr, P.J., B.N. Taylor, and D.B. Newell, 2011, *The 2010 CODATA Recommended Values of the Fundamental Physical Constants (Web Version 6.0)*, Available: http://physics.nist.gov/constants, National Institute of Standards and Technology, Gaithersburg, MD 20899.

Munson, D.E., 1998. *Analysis of Multistage and Other Creep Data for Domal Salts*, SAND98-2276**,** Sandia National Laboratories, Albuquerque, NM

Park, B.Y., B.L. Ehgartner, M.Y. Lee, and S.R. Sobolik, 2005. *Three Dimensional Simulation for Big Hill Strategic Petroleum Reserve (SPR),* SAND2005-3216, Sandia National Laboratories, Albuquerque, NM.

Rautman, C.A. and A.S. Lord, 2007. *Sonar Atlas of Caverns Comprising the U.S. Strategic Petroleum Reserve Volume 2: Big Hill Site, Texas*, SAND2007-6023, Sandia National Laboratories, Albuquerque, NM.

Rautman, C.A., and B.L. Ehgartner, 2004. *Pillar to Diameter Ratios for Big Hill,* Letter from C. Rautman and B. Ehgartner to R.E. Myers, DOE SPR PMO dated February 23, 2004.

Shipton, Z.K., A.M. Soden, J.D. Kirkpatrick, A.M. Bright, and R.J. Lunn, 2006. *How thick is a fault? Fault displacement-thickness scaling revisited. In Abercrombie,* R. (Eds) Earthquakes: Radiated Energy and the Physics of Faulting, pages pp. 193-198, AGU.

Wawersik, W.R. and D.H Zeuch, 1984. *Creep and Creep Modeling of Three Domal Salts – A Comprehensive Update,* SAND84-0568, Sandia National Laboratories, Albuquerque, NM.

APPENDIX I: BIG HILL LOGGING RESULTS WITH THE WEATHERFORD MULTI ARM CALIPER

Big Hill Logging Results with the Weatherford Multi Arm Caliper Tasks 1.1.4 Activity a2 and Task 1.1.6 activity a1

Allan Sattler and Brian Ehgartner

Introduction

This report summarizes some of the results of the casing inspection report of the Weatherford Multi Arm Caliper Log in the fourteen 14 Big Hill (BH) slick "A" wells and in BH 105 and 109 B wells. We attempt to put these results on a consistent quantitative basis by examination of three parameters derived from Weatherford's T Vison, strain, ovality, and shear deformation. Ovality and strain are calculated in the TVision Formalism and are displayed and defined below:

- The Ovality Track presents the results of the TVisionSE ovality analysis. Ovality represents the degree of irregularity of the circular section, quantified by the difference in largest and smallest cross-section axes.
- The Strain Track is used to present the results of the TVisionSE strain analysis. The strain is calculated as amount of casing strain required to produce the deformations presented in the Trajectory Track and Ovality Tracks.
  The Trajectory Track is used to present the results of the TVisionSE trajectory analysis. The trajectory results are indicative of distance that the centre of the casing is from the position calculated from a well survey, or in case where no well survey is available, from the position the centre of the casing should be based on the cumulative results of the trajectory analysis.

These calculated values are useful however for comparison of the logging results of one casing string to another, putting it on a consistent basis. Ovality can be read directly. There is in T Vision a shear calculation which is not presented in the supplied format. In this case, shear was measured directly from the ovality track by magnifying the horizontal deviation and measuring it directly in inches. The horizontal displacement in inches was divided by the number of feet of pipe over which the deviation was measured. The shear was calculated for the respective salt/caprock interface horizons for BH cavern well casings.

This note highlights the results of shear, strain and ovality at the BH salt caprock interface for these 16 BH wells. This note also mentions results on ovality at other horizons. The results at the salt caprock interface can be displayed in pseudo 2D for these cavern well casings because the depth is effectively frozen around 1620-1640 ft, which is the interval of the salt/caprock interface over these cavern wells.

The analysis was done from the original Weatherford T Vision displays and the analysis of the trajectory data for shear. Generally, the most critical BH horizons over this body of well casings are at the salt/caprock interface although results from other BH horizons are quite intriguing.

This short note covers:

(1) Shear, strain, and ovality results for the BH salt caprock interface
(2) Inferences of the condition of the 20-in casing from the shear data
(3) Additional correlations derived from the ovality data

Shear, strain and ovality results for the BH salt-caprock interface

The results of shear measurements/calculations are shown in Figure 1. The summary of the shear, strain, and ovality at the salt caprock interface is shown in Table 1. Table 1 is color coded to show relative severity of shear, ovality, and strain. Table 1 presents a pseudo 2D picture of these quantities at the salt caprock interface. The results are laid out in the same geometric order as the BH wells. Reported data on orientation are inaccurate and should be ignored.

BH Cavern Wells 101 A, 102 A, and 110 A are shown to be rather well behaved in the horizons of the salt caprock interface, Table 1. The values of the shear quantities are relatively low and the observed values of strain and ovality are also low. In the case of BH 110 A however, the observed strain is in the medium range. Most certainly there is no rupture at these horizons. These three quantities, shear, ovality and strain in the case of caverns 107A, 108 A, and 112 A are somewhat higher, Table 1. Their casings generally manifest more deformation at the salt caprock than the group of casings above but their casings appear integral, no rupture at these horizons. At this time relatively little concern for casing damage at these horizons. Some of these quantities in the case of BH Cavern Wells 103A, 104 A, 105 A, 106 A, and 109 A are in and 111 A are in the high range. There are no ruptures, casing is integral but these wells bear watching. BH wells 105 A, 106 A, and 109 A have quite large metal losses but this is attributed more to ovality than erosion or corrosion.

The BH cavern well casings 105 B, 113 A, 109 B, and 114 A have problems, Table 1. BH 105 B has been badly deformed and the casing apparently was penetrated. Strain, shear, and ovality quantities measured from the log are very high. The caliper suggests that the 114 A well has been penetrated but no leak has been observed. Strains and ovality are very high and relative strain is high. The BH 113 A production casing hasn't been penetrated but the deformation is quite marked. The strain observed from T Vision is very high, the shear and relative strain are high. BH 113A and 114 A are on the "watch" list. Cavern 105 B and 109 B already have liners.

The 20-inch casing, what can be inferred about it shape from the shear calculation?

One can only surmise the shape of the 20-in casing in some of the WH cavern wells. Those 20-inch casings lying outside the cavern wells where the shear was the highest are most likely to be very suspect i. e. breached! Those are Cavern Wells 105 B where the shear was very high and likely Cavern wells 104 A, 105 A, 106 A, 113 A where the shear is high. Shear deformation of the production casing is significant in these cases. It is difficult to see how the 20-inch casings of the cavern wells mentioned just above could be integral and, at the same time, permit such deformation to the production string inside.

Additional correlations from the ovality readout

To get an idea of the additional correlations, the data in Table 2 is the same format as Table 1, i. e. a pseudo two dimensional display with approximate 2D ordering of the wells. Table 2 displays the cavern well casings where the measured ovality is greater than 0.1- inch, in four or more instances, in the one hundred foot segments of the 300-900-ft interval. This is generally in the interval of the gypsum caprock. From Table 3 it is observed that is little ovality > 0.1-inch in the body of the BH well casings from ~900-ft 1500-ft. This interval encompasses the "anhydrite portion" of the caprock and the top bottom of the gypsum portion. These are areas where there are generally two casings the 13- 3/8 production casing and

the 20-in casing. There seems to be little ovality > or = to 0.1-in below 300 ft but that could be influenced by the added presence of the 30-in casing. The 30-in casing's depth in the BH cavern wells ranges from ~300-600 ft. Below 1700 ft, in the salt itself, there is a fair amount of ovality > or =0.1-inch in the body of the cavern well casings. There is just the 13-3/8-in production casing over most of that interval as the 20-inch casing only extends ~100-200 ft into the salt. At the salt/caprock interface, just over 1600-ft, there is obviously ovality as shown in Table 1. It is remarkable that ovality > or = 0.1-inch manifest itself in some instances through two or three casings.

Conclusion

The shear, ovality and strain readouts of the T Vision format seem to be a reasonable systematic semi quantitative way to display much of the T Vision output from the Weatherford's Multi Arm Caliper. The shear also can be derived directly from a blowup display of the trajectory. These statements seem to hold at least in the data from BH casings displayed so far. Once the seismic data is analyzed better correlations of with the casing deformation are very probable. These data should also serve in the more global BH modeling of the casing damage. It is remarkable that casing deformation of the production string manifests itself in through one or even two outer casings.

Figure 1, BH Dog-legs at Salt/Caprock Interface Data from Weatherford Multi Arm Caliper

Table 1, BH Shear, Strain and ovality at the Salt/Caprock Interface Data from Weatherford Multi Arm Caliper

well	105a	105b	104a	103a	102a	101
horizontal displacement in	1.09	1.20	0.74	0.38	0.41	0.68
vertical distance ft	8.5	4	5.3	4.5	10	14
shear in/ft	0.13	0.30	0.14	0.08	0.04	0.05
relative strain	med	very high	high	high	low	low
micro strains	8	>20	~, <12	7	0	3
ovality, in	0.3	>0.5	0.2	0.1	0.1	0.1
orientation deg	12	-6	276	0	132	6

well	110a	109a	109b	108a	107a	106a
horizontal displ. in	0.12	0.44		0.44	0.49	0.90
vertical distance ft	3	5.5		5	7	7
shear in/ft	0.04	0.08		0.09	0.07	0.13
relative strain	med	high		med	med	high
micro strains	4	15	12	6	5	11
ovality , in	0.1	0.35	.038	0.3	0.2	0.2
orientation deg	-18	-324		114	54	24

well	114a	113a	112a	111a
horizontal displacement in	1.01	1.15	0.38	0.80
vertical distance ft	11	9	8	9
shear in/ft	0.09	0.13	0.05	0.09
relative strain	high	high	med	high
micro strains	>20	18	7	8
ovality , in	>0.5	0.25	0.25	0.35
orientation deg	138	180	246	162

KEY

	range of shear		microstrains		ovality	
low	0	0.05	0	5	0	0.15
medium	0.05	0.1	5	10	0.15	0.3
high	0.1	0.15	10	20	0.3	0.5
very high	>0.3		>20		>.5	

bold indicates failed well integrity (BH105b and 109b)

Table 2, BH Ovality Greater then ~0.1-in four or more 100-ft segments in the 100 to 900 ft Horizons (highlighted) Data from Weatherford Multi Arm Caliper

well	105a	105b	104a	103a	102a	101
horizontal displacement in	1.09	1.20	0.74	0.38	0.41	0.68
vertical distance ft	8.54		5.3	4.5	10	14
shear in/ft	0.13	0.30	0.14	0.08	0.04	0.05
relative strain	med	very high	high	high	low	low
micro strains	8	>20	~, <12	7	0	3
ovality, in	0.3	>0.5	0.2	0.1	0.1	0.1
orientation deg	12	-6	276	0	132	6

well	110a	109a	109b	108a	107a	106a
horizontal displ. in	0.12	0.44		0.44	0.49	0.90
vertical distance ft	3	5.5		5	7	7
shear in/ft	0.04	0.08		0.09	0.07	0.13
relative strain	med	high		med	med	high
micro strains	4	15	12	6	5	11
ovality , in	0.1	0.35	.038	0.3	0.2	0.2
orientation deg	-18	-324		114	54	24

well	114a	113a	112a	111a
horizontal displacement in	1.01	1.15	0.38	0.80
vertical distance ft	11	9	8	9
shear in/ft	0.09	0.13	0.05	0.09
relative strain	high	high	med	high
micro strains	>20	18	7	8
ovality , in	>0.5	0.25	0.25	0.35
orientation deg	138	180	246	162

Table 3 100-ft horizon segments containing ovality that is >0.1in

Well	101 A	102 A	103 A	104 A	105 A	105 B	106 A	107 A	108 A	109 A	109 B	110 A	111 A	112 A	113 A	114 A
100						x										x
200										x						x
300									x	x	x	x		x		
400				x		x			x	x	x	x		x		
500				x						x	x	x		x		
600				x						x	x	x		x		
700		x		x		x				x	x	x		x		
800		x	x	x									x		x	
900			x			x										
1000																
1100																x
1200															x	
1300															x	
1400												x				
1500	x											x				x
1600	x	x	x	x	x	x	x	x	x	x	x	x	x	x	x	x
1700		x		x	x	x		x	x	x	x	x	x			x
1800	x	x		x	x	x	x	x	x	x	x	x	x	x		x
1900	x		x	x	x		x	x	x	x	x		x	x		x
2000	x	x	x		x	x	x	x			x		x		x	X
2100		x														
2200																
2300																
2400																

DISTRIBUTION

1 U.S. Department of Energy
Attn: D. Johnson, FE-40
Deputy Assistant Secretary for Petroleum Reserves
1000 Independence Avenue SW
Washington, D.C. 20585

1 US Department of Energy
Attn: Deputy Director, RW-2
Office of Civilian Radioactive Waste Mgmt.
Forrestal Building
Washington, DC 20585

Electronic copy only to Jerry Berndsen at Gerard.berndsen@spr.doe.gov for distribution to DOE and DM

1	MS0372	J. G. Arguello Jr.	1525
1	MS0824	J. E. Bean	1525
1	MS0706	D. J. Borns	6912
1	MS0706	B. L. Ehgartner	6912
1	MS0706	D. L. Lord	6912
1	MS0706	Anna C.S. Lord	6912
1	MS0735	J. A. Merson	6910
1	MS0751	R. E. Finley	6911
5	MS0751	B. Y. Park	6914
1	MS1033	S. J. Bauer	6914
1	MS0751	S. R. Sobolik	6914
1	MS1395	C. G. Herrick	6211
1	MS1395	M.Y. Lee	6211
1	MS0899	Technical Library	9532 (electronic copy)
1	MS0731	823 Library	10662


Sandia National Laboratories